

Doctoral thesis

High Energy Particle Collision
and Energy Extraction Process
near a Rotating Black Hole

回轉ブラックホール近傍における
高エネルギー粒子衝突とエネルギー引き抜き過程

Kota Ogasawara

Department of Physics, Graduate School of Science,
Rikkyo University

Abstract

We consider a collision of two geodesic particles and dust thin shells with a high center-of-mass (CM) energy in the Bañados-Teitelboim-Zanelli spacetime. We show that the CM energy of both the particles and shells can be arbitrarily large if either of the colliding objects satisfies a certain critical condition.

The rest mass and energy of colliding objects are usually assumed to be sufficiently small compared to the mass of the background black hole. However, if the CM energy becomes comparable with the gravitational energy of the black hole, the self-gravity of colliding objects cannot be neglected. An analytical treatment of the self-gravity effects on the particle collision is much complicated and difficult but it is easily possible in the shell collision.

We compare the dust thin shell collision and the particle collision in order to investigate the effects of the self-gravity of colliding objects on the high energy collision. The self-gravity of the shells affects the position of an event horizon and it covers the high energy collisional event. Therefore, we conclude that the self-gravity of colliding objects suppresses its CM energy and that any observer who stands outside of the event horizon cannot observe the collision with an arbitrary high CM energy. We find a test shell limit, where the CM energy and the effective potentials for shells in the limit are very similar to the ones of particles. The test shell limit would help us to understand the effect of the self-gravity of the thin shells on the collisions.

We also investigate a particle collision and energy extraction in the Kerr spacetime. We consider the reaction of particles 1 and 2 into particles 3 and 4 in the ergoregion, where particle 3 escapes to infinity after the collision, while particle 4 falls into the black hole possibly with negative energy due to the existence of the ergosphere. If the energy of particle 4 is negative, the energy of the escaping particle can be larger than the total energy of the injected particles because of energy conservation. The energy extraction efficiency is defined as the energy ratio of the escaping particle to the injected particles.

We present an analytic formulation to investigate the energy extraction efficiency and the escape probability. We consider a collision of two particles which started from infinity and follow geodesics in the equatorial plane. We focus on a collision with arbitrarily large CM energy, which occurs if either of the colliding particles satisfies a certain critical condition. We show that if this particle is ingoing on the collision, the upper limit of the efficiency is $(2 + \sqrt{3})(2 - \sqrt{2}) \simeq 2.186$, while if it is bounced back before the collision, the upper limit of the efficiency is $(2 + \sqrt{3})^2 \simeq 13.93$.

Focusing on more general head-on collisions, where one of the two colliding particles is generated in the ergoregion and initially moves outwardly, we show that a produced massless particle can escape to infinity with arbitrarily large energy in the near-horizon limit of the collision point. Furthermore, if we assume that the emission of the produced massless particles is isotropic in the

center-of-mass frame but confined to the equatorial plane, the escape probability approaches $5/12$ and almost all escaping particles have arbitrarily large energy at infinity.

Contents

1	Introduction	3
2	Kerr black holes as particle accelerators and energy sources	8
2.1	Geodesic motion in the Kerr spacetime	8
2.1.1	Kerr metric	8
2.1.2	General geodesic	10
2.2	Kerr black holes as particle acceletators	11
2.2.1	Particle collision in the equatorial plane	11
2.2.2	BSW process	12
2.3	Energy extraction process	13
2.3.1	Penrose process	14
2.3.2	Collisional and super-Penrose process	15
3	High energy particle collision near a BTZ black hole	16
3.1	Particle motion in the BTZ black hole	16
3.1.1	BTZ spacetime	16
3.1.2	General geodesic of a particle	17
3.1.3	Motion of a critical particle	19
3.1.4	Motion of a subcritical particle	20
3.2	CM energy for particle collisions	21
3.2.1	General colliding particles	21
3.2.2	Critical angular momentum limit	22
4	Collision of two thin shells in the BTZ spacetime	24
4.1	Collision of two particles with vanishing angular momenta	24
4.2	Thin shell and its motion in the BTZ spacetime	26
4.3	Collision of two dust thin shells	31
4.3.1	CM energy	33
4.3.2	Observable CM energy	35
4.3.3	Test shell limit	35
5	Collisional Penrose process	37
5.1	Particle motion in the Kerr black hole	37
5.1.1	Geodesic in the equatorial plane	37

5.1.2	Radial turning points	38
5.2	Particle collision and reaction	39
5.2.1	Particle collision on the horizon	40
5.2.2	Near horizon and near critical behaviors	41
5.2.3	Expansion of the radial momentum	42
5.3	Energy extraction efficiency	43
5.3.1	First order of the radial momentum conservation	43
5.3.2	Second order of the radial momentum conservation	44
5.3.3	Maximum efficiency	45
6	Arbitrarily large energy extraction and escape probability	47
6.1	Particle collision and escape cone	47
6.2	Super-Penrose process and escape probability	51
7	Conclusions	55

Chapter 1

Introduction

In 2009, Bañados, Silk, and West (BSW) [1] pointed out that the center-of-mass (CM) energy of two colliding particles can be arbitrarily large, if the collision occurs near the event horizon of an extremal Kerr black hole and either of the colliding particles satisfies a certain critical condition. This is now called “BSW process” or “BSW collision”.

In fact, a particle collision with an arbitrarily large CM energy had already been noticed by Piran, Shaham, and Katz [2] in the study of energy extraction from a rotating black hole by using a particle collision, which is called “collisional Penrose process”. See Harada and Kimura [3] and Schnittman [4] for a brief review and references therein for further details.

A lot of high energy phenomena in the universe, such as ultra-high-energy cosmic rays and jets from AGN, have been observed. However, there are still unknown physics about these acceleration mechanisms. Terrestrial particle accelerators, such as the Large Hadron Collider, and leading mechanisms of particle acceleration proposed by astrophysics make use of electromagnetic interaction for charged particles.

Recently, the first detection of gravitational waves has been reported by the LIGO Scientific and the Virgo Collaborations [5], the existence of black holes was ensured in our universe. Since black holes have strong gravity and this gravitational force works on both charged and neutral particles, black holes can accelerate not only charged particles but also neutral particles. The phenomena in a strong gravitational field near black holes such as the BSW process and the collisional Penrose process would be important in astronomy and astrophysics. If the BSW process works, the energy of the particle collision can reach Planck-scale and it can probe the physics of Planck-scale by observing near the event horizon black holes. In addition, if the collisional Penrose process works, black holes can be the origins of ultra-high-energy cosmic rays and energy sources of jets from AGN, etc.

After the rediscovery by Bañados *et al.* [1], several critical comments on the BSW process were given in Refs. [6, 7, 8]. We pick up following relevant ones: Although a spin parameter for astrophysical black holes has an upper bound $a \leq 0.998M$,¹ the BSW process requires the extremal Kerr black hole, i.e., $a = M$. The conserved energy and angular momentum of either of two colliding particles must be fine tuned-to the critical condition. It needs arbitrarily long proper time for a particle, which satisfies the critical condition, to reach the event horizon for a maximally rotating black hole. A self-gravity of colliding particles and an emission of gravitational waves would significantly affect the BSW process.

The details of the BSW process have been investigated to answer the criticisms. Harada and Kimura showed that the critical condition is naturally realized in a collision of an innermost stable circular orbit particle in an extremal Kerr black hole [10] and estimated a bounded CM energy on a particle collision including the effect of emission of gravitational waves [11]. Patil *et al.* [12] considered a finite CM energy of a collision of two particles with a finite proper time. The BSW process has been further investigated in a nonequatorial plane of a Kerr black hole [13], a weak electromagnetic field [14], and the near-horizon geometry of an extremal Kerr spacetime [15].

The particle collision with a high CM energy occurs not only in a Kerr black hole spacetime but also in a Kerr naked singularity spacetime [16], a Kerr-Newmann spacetime [17], a Kerr-(anti-)de Sitter spacetime [18], lower-dimensional spacetimes [19, 20, 21, 22, 23, 24], and higher dimensional spacetimes [25, 26]. As the electromagnetic counterpart of the BSW process, a charged particle collision with a high CM energy has been investigated in an extremal Reissner-Nordström spacetime [27] and in a higher-dimensional Reissner-Nordström spacetime or an electrical charged Myers-Perry spacetime [28].

The rest mass and energy of each colliding particle are usually assumed to be sufficiently small compared to the mass of the background black hole. However, if the CM energy becomes comparable with the gravitational energy of the black hole, the self-gravity of colliding particles cannot be neglected. The self-gravity caused by the high-energy collision will affect the BSW process and the CM energy will be limited to a finite value. Unfortunately, it is much complicated and difficult to treat the self-gravity effects on a particle collision.

Kimura *et al.* [29, 30, 31] considered a collision of two thin shells in a Reissner-Nordström spacetime instead of a Kerr spacetime for simplicity. They calculated a collision of two shells including their self-gravity and estimated the upper limit of the CM energy of the shell collision analytically.

Can we treat a shell collision in stationary and axisymmetric spacetime? The analytical treatment of the shell collision in the Kerr spacetime is very difficult [32, 33] but the difficulty of the technical problem depends on the dimension of

¹ This is called Thorne's bound [9]. Thorne's bound is based on the standard accretion disk model. The spin parameter is related to the angular momentum with respect to the rotational axis as $J = Ma$, where J and M are the angular momenta and mass parameters of a Kerr spacetime, respectively.

the spacetime [34, 35, 36]. Mann *et al.* [34] investigated the collapse of a shell in a 2 + 1 dimensional stationary and axisymmetric spacetime and they showed that the motion of the shell in 2 + 1 dimension is tractable. Note that again the BSW collision occurs not only in 4-dimensional spacetimes but also in lower and higher dimensional spacetimes. Therefore, it would be worth considering a collision of two thin shells in lower and higher dimensional spacetimes.

A black hole solution in 2 + 1 dimension was obtained by Bañados, Teitelboim, and Zanelli (BTZ) [37, 38]. The BTZ black hole is considered as a typical black hole in 2 + 1 dimension because of the existence of a no-go theorem for asymptotically flat and stationary black holes satisfying the dominant energy condition in 2+1 dimensions in Einstein gravity [39]. One may suspect that the negative cosmological constant affects the particle collision, and it is very different from the BSW process in the Kerr spacetime. The effect of the negative cosmological constant on the BSW process will be negligible since the collision with the high CM energy occurs near an extremal event horizon.

In the BTZ spacetime, particle motions [40], the BSW collision [19, 20, 21, 24], gravitational perturbations induced by falling particles [41], and thermodynamics of thin shells [42, 43, 44] have been investigated.

The high CM energy collision of particles can produce high energy and/or very massive particles. We should keep in mind that an observer distant from a black hole may not see particles with high energy and/or very massive even if the CM energy is very large because the produced particles must be highly red-shifted. If such energetic particles can escape to infinity, extra energy gain is necessary. In this context, it is known that the rotating energy of black holes can be extracted. For this process, the existence of ergoregion, where the energy of the particle E^2 can be negative, plays an important role.

In 1969, Penrose [45] pointed out the energy extraction process by using particle division, which is called “Penrose process”. Since we are interested in the energy extraction by using the particle collision, let us consider a collision of two particles. This process, i.e., the collisional Penrose process [2, 46], is typically as follows.

We consider the reaction of particles 1 and 2 into particles 3 and 4 in the ergoregion, where particle 3 escapes to infinity after the collision, while particle 4 falls into the black hole possibly with negative energy due to the existence of the ergosphere. For each particle i ($i = 1, 2, 3, 4$), we write E as E_i . In this case, if the energy of particle 4 E_4 is negative, we have

$$E_3 = E_1 + E_2 - E_4 > E_1 + E_2, \quad (1.1)$$

where we have used the energy conservation equation. The energy extraction

² If spacetime has the time-translational Killing vector ξ^μ , the energy of particle E is defined as $E \equiv -\xi^\mu p_\mu$, where p^μ is the 4-momentum of the particle.

efficiency η in the collisional Penrose process is defined as

$$\eta \equiv \frac{\text{energy of the escaping particle}}{\text{total energy of the injected particles}} = \frac{E_3}{E_1 + E_2}. \quad (1.2)$$

The energy extraction ($\eta > 1$) from the black hole is possible provided $E_4 < 0$.

Recently, the interplay between the particle acceleration and energy extraction has been intensively investigated by several authors. Bejger *et al.* [47] showed that the maximum efficiency only amounts to about 1.4 for rear-end collisions if either of the colliding particles satisfies a certain critical condition. This result was confirmed analytically by Harada *et al.*, [48]. However, Schnittman [49] numerically showed that the maximum efficiency can reach about 14 for head-on collisions, which is exactly given by $(2 + \sqrt{3})^2$ [50, 51, 52]. Berti, Brito, and Cardoso [53] showed that an arbitrarily large efficiency is possible by more general head-on collisions, which is called “super-Penrose process”. In the super-Penrose process, a radially outward particle must be created near the horizon by some preceding process. An escape probability of the produced particle has been investigated in an extremal Kerr black hole spacetime [54] and in a Kerr naked singularity spacetime [55].

This thesis is organized as follows:

Chapter 2

We briefly review the general geodesic motion, BSW process, and Penrose process in the Kerr black hole spacetime.

Chapter 3

We consider a particle collision in the BTZ black hole spacetime with the negative cosmological constant and angular momentum motivated by next investigations. This is based on

N. Tsukamoto, K. Ogasawara, and Y. Gong, “Particle collision with an arbitrarily high center-of-mass energy near a Bañados-Teitelboim-Zanelli black hole,” *Phys. Rev. D* **96**, 024042 (2017) [24].

Chapter 4

We consider a collision of two dust thin shells in the BTZ spacetime and compare the shell collision and the particle collision in order to investigate the effects of the self-gravity of colliding objects on the high CM energy collision. This is based on

K. Ogasawara and N. Tsukamoto, “Effect of the self-gravity of shells on a high energy collision in a rotating Bañados-Teitelboim-Zanelli spacetime,” *Phys. Rev. D* **99**, 024016 (2019) [56].

Chapter 5

We present an analytic formulation to investigate the upper limits of the energy of the escaping particle and of the energy extraction efficiency in the collisional Penrose process. This is based on

K. Ogasawara, T. Harada, and U. Miyamoto, “High efficiency of collisional Penrose process requires heavy particle production,” *Phys. Rev. D* **93**, 044054 (2016) [51] and

T. Harada, K. Ogasawara, and U. Miyamoto, “Consistent analytic approach to the efficiency of collisional Penrose process,” *Phys. Rev. D* **94**, 024038 (2016) [52].

Chapter 6

We also present an analytic formulation to investigate an arbitrarily large energy extraction and escape probability in the super-Penrose process. This is based on

K. Ogasawara, T. Harada, U. Miyamoto, and T. Igata, “Escape probability of the super-Penrose process,” *Phys. Rev. D* **95**, 124019 (2017) [54].

Chapter 7

We show the conclusions of this thesis.

In this thesis, we use the units in which the speed of light is unity. We set Newton’s constant in four dimensions unity except for Chaps. 3 and 4. We set $8G = 1$ in Chaps. 3 and 4 as in Sec. III in Ref. [34], where G is Newton’s constant in three dimensions.

Chapter 2

Kerr black holes as particle accelerators and energy sources

In this Chapter, we investigate the general geodesic motion of the particle in the Kerr black hole and make a brief review of the BSW process [1] and the Penrose process [45].

2.1 Geodesic motion in the Kerr spacetime

2.1.1 Kerr metric

The line element $ds^2 = g_{\mu\nu}dx^\mu dx^\nu$ in the Kerr spacetime [57] in the Boyer-Lindquist coordinates is given by

$$ds^2 = - \left(1 - \frac{2Mr}{\rho^2}\right) dt^2 - \frac{4Mar \sin^2 \theta}{\rho^2} dt d\varphi + \frac{\rho^2}{\Delta} dr^2 + \rho^2 d\theta^2 + \left(r^2 + a^2 + \frac{2Ma^2r \sin^2 \theta}{\rho^2}\right) \sin^2 \theta d\varphi^2, \quad (2.1)$$

where

$$\rho^2 \equiv \rho^2(r, \theta) = r^2 + a^2 \cos^2 \theta, \quad (2.2)$$

$$\Delta \equiv \Delta(r) = r^2 - 2Mr + a^2. \quad (2.3)$$

The spacetime is parametrized by two parameters, namely mass M and spin a . The spin parameter is related to the angular momentum J with respect to the rotational axis of the black hole as $a = J/M$. We note that the metric,

given by Eq. (2.1), reduces to the Schwarzschild black hole spacetime if the spin parameter vanishes, i.e., $a = 0$.

The Kerr spacetime is stationary and axisymmetric with corresponding two Killing vectors ξ^μ and ψ^μ , where $\xi^\mu \partial_\mu = \partial_t$ and $\psi^\mu \partial_\mu = \partial_\varphi$. We assume $a \geq 0$ without loss of generality because taking $\varphi \rightarrow -\varphi$ effectively changes the sign of a . When $a \leq M$ is satisfied the spacetime has an event horizon at

$$r = r_+ \equiv M + \sqrt{M^2 - a^2}, \quad (2.4)$$

where $\Delta(r)$ vanishes at $r = r_+$, and it is known as an extremal black hole for $a = M$. For $a > M$, it has a naked singularity at $r = 0$ and $\Delta(r) = 0$ has no real roots.

Although the time translation Killing vector ξ^μ is timelike at infinity, it need not be timelike everywhere outside of the event horizon. The norm of ξ^μ is given by

$$\xi^\mu \xi_\mu = g_{tt} = - \left(1 - \frac{2Mr}{r^2 + a^2 \cos^2 \theta} \right), \quad (2.5)$$

so ξ^μ is nontimelike when

$$r^2 - 2Mr + a^2 \cos^2 \theta \leq 0, \quad (2.6)$$

is satisfied. The boundary of this region, i.e., the hypersurface

$$r = r_E \equiv M + \sqrt{M^2 - a^2 \cos^2 \theta}, \quad (2.7)$$

is the ergosphere. The ergosphere intersects the event horizon at $\theta = 0$ and π . The region, where ξ^μ becomes spacelike is called ergoregion. See Fig. 2.1 for the schematic picture.

We find that the vector

$$\chi^\mu \equiv \xi^\mu + \Omega_H \psi^\mu, \quad (2.8)$$

is null on the event horizon, where

$$\Omega_H \equiv \left. \frac{d\varphi}{dt} \right|_{r=r_+} = \frac{a}{r_+^2 + a^2} = \frac{a}{2M(M + \sqrt{M^2 - a^2})}, \quad (2.9)$$

is the angular velocity of the event horizon. Because it is a linear combination of two Killing vectors ξ^μ and ψ^μ , χ^μ is also a Killing vector and a null generator of the event horizon. We note a difference between a static (Schwarzschild) and stationary (Kerr) black hole. For a static black hole, ξ^μ becomes null on the event horizon. For a stationary black hole, ξ^μ becomes null on the ergosphere and χ^μ becomes null on the event horizon.

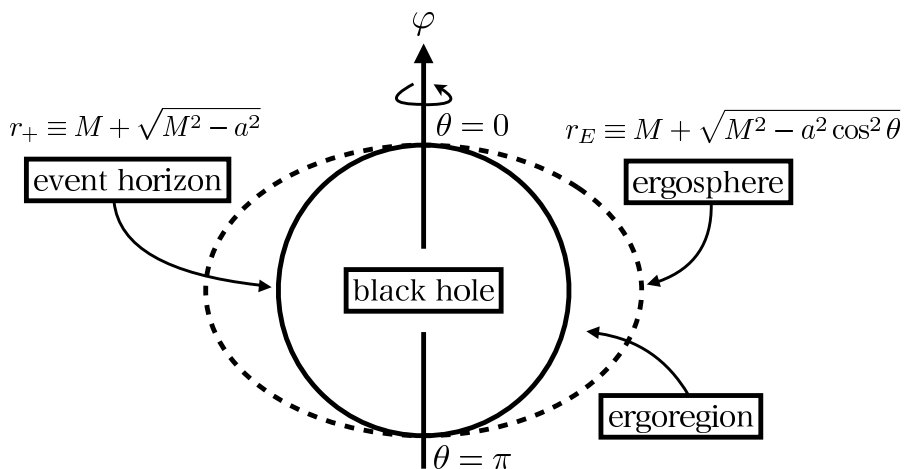


Figure 2.1: The schematic picture showing a side view of the Kerr black hole. The radial position of the event horizon and ergosphere are given by $r_+ \equiv M + \sqrt{M^2 - a^2}$ and $r_E \equiv M + \sqrt{M^2 - a^2 \cos^2 \theta}$, respectively. The ergosphere intersects the event horizon at $\theta = 0$ and π . The region $r_+ < r < r_E$, where the Killing vector ξ^μ becomes spacelike, is called the ergoregion.

2.1.2 General geodesic

The conserved energy E and angular momentum L of a particle with the 4-momentum p^μ are defined as

$$E \equiv -g_{\mu\nu} \xi^\mu p^\nu, \quad (2.10)$$

and

$$L \equiv g_{\mu\nu} \psi^\mu p^\nu, \quad (2.11)$$

respectively. These two conserved quantities are constant along a geodesic for the particle. Furthermore, there exists an additional constant \mathcal{Q} , which is known as a Carter constant. Because the sufficient number of constants of motion, the equations of motion of this system are completely integrable.

By using the Hamilton-Jacobi method [58], the components of the 4-momentum

are given by

$$p^t = \frac{1}{\rho^2} \left[-a(aE \sin^2 \theta - L) + \frac{(r^2 + a^2)P}{\Delta} \right], \quad (2.12)$$

$$p^r = \frac{\sigma}{\rho^2} \sqrt{R}, \quad (2.13)$$

$$p^\theta = \frac{\sigma^\theta}{\rho^2} \sqrt{\Theta}, \quad (2.14)$$

$$p^\varphi = \frac{1}{\rho^2} \left[- \left(aE - \frac{L}{\sin^2 \theta} \right) + \frac{aP}{\Delta} \right], \quad (2.15)$$

where $\sigma \equiv \text{sgn}(p^r)$, $\sigma^\theta \equiv \text{sgn}(p^\theta)$,

$$P \equiv (r^2 + a^2)E - aL, \quad (2.16)$$

$$\Theta \equiv \mathcal{Q} - \cos^2 \theta \left[a^2(m^2 - E^2) + \frac{L^2}{\sin^2 \theta} \right], \quad (2.17)$$

$$R \equiv P^2 - \Delta [m^2 r^2 + (L - aE)^2 + \mathcal{Q}], \quad (2.18)$$

and m denotes a rest mass of the particle.

2.2 Kerr black holes as particle acceletators

If two particles 1 and 2 are at the same spacetime point, the energy observed by an observer whose 4-velocity is parallel to the sum of 4-momenta p_1^μ and p_2^μ of two particles 1 and 2, respectively, at that point is the center-of-mass (CM) energy. The CM energy is defined as

$$E_{\text{cm}}^2 \equiv -g_{\mu\nu} (p_1^\mu + p_2^\mu) (p_1^\nu + p_2^\nu), \quad (2.19)$$

where $g_{\mu\nu}$ is the spacetime metric. We concentrate on a collision of two particles that come from infinity.

2.2.1 Particle collision in the equatorial plane

We consider the situation where two particles move inward on the equatorial plane and collide rear-end near the event horizon. In this case, the CM energy for a near-horizon collision is given by [10, 11]

$$\begin{aligned} \lim_{r \rightarrow r_+} E_{\text{cm}}^2 = & m_1^2 + m_2^2 + \frac{m_1^2 r_+^2 + (L_1 - aE_1)^2}{r_+^2} \frac{E_2 - \Omega_H L_1}{E_1 - \Omega_H L_2} \\ & + \frac{m_2^2 r_+^2 + (L_2 - aE_2)^2}{r_+^2} \frac{E_1 - \Omega_H L_2}{E_2 - \Omega_H L_1} - \frac{2(L_1 - aE_1)(L_2 - aE_2)}{r_+^2}, \end{aligned} \quad (2.20)$$

where E_i , L_i , and m_i are E , L , and m for particle i ($i = 1, 2$), respectively. Therefore, the CM energy is divergent if either of particles 1 and 2 satisfies

a condition $E_i - \Omega_H L_i = 0$. We call the condition $E_i - \Omega_H L_i = 0$ a critical condition, and particles which satisfy the critical condition are called critical particles. When both the particles satisfy the critical condition, the CM energy in the near horizon becomes finite.

For such a high energy collision to occur, the critical particle must reach the near horizon from infinity. We concentrate on a geodesic motion of a massive particle in the equatorial plane. From Eq. (2.13), it reduces to a simple one-dimensional potential problem as

$$\frac{1}{2} (p^r)^2 + V(r) = 0, \quad (2.21)$$

where

$$V(r) = -\frac{Mm^2}{r} + \frac{L^2 - a^2 (E^2 - m^2)}{2r^2} - \frac{M(L - aE)^2}{r^3} - \frac{E^2 - m^2}{2}, \quad (2.22)$$

is the effective potential for the particle.

For simplicity, we consider a particle which is initially at rest at infinity, i.e., $E = m$. In this case, a particle which satisfies a condition

$$2r^2 - Ml^2 r + 2M^2(l - a_*)^2 > 0, \quad (2.23)$$

can approach the event horizon from infinity, where $l \equiv L/(Mm)$ and $a_* \equiv a/M$. Solving this condition for l , we obtain

$$-2(1 + \sqrt{1 + a_*}) \equiv l_L < l < l_R \equiv 2(1 + \sqrt{1 - a_*}). \quad (2.24)$$

We introduce a nondimensional critical angular momentum $l_c \equiv E/(\Omega_H Mm)$ as the critical value of l . The explicit form of l_c with $E = m$ is given by

$$l_c = \frac{2(1 + \sqrt{1 - a_*})}{a_*}. \quad (2.25)$$

We note that $l_R \leq l_c$ and equality holds only for $a_* = 1$. This implies that the critical particle can approach the event horizon for $a_* = 1$ but cannot for $a_* < 1$.

2.2.2 BSW process

We consider a particle motion with the 4-velocity u^μ and a rest mass m in the equatorial plane $\theta = \pi/2$ of the Kerr black hole. The conserved specific energy and angular momentum of the particle are given by

$$e \equiv -g_{\mu\nu} \xi^\mu u^\nu \quad \text{and} \quad \ell \equiv g_{\mu\nu} \psi^\mu u^\nu, \quad (2.26)$$

respectively. Using these constants of motion and the normalization condition of the 4-velocity, $g_{\mu\nu}u^\mu u^\nu = -1$, the components of the 4-velocity are given by

$$u^t = \frac{1}{r^2} \left[\frac{(r^2 + a^2)T}{\Delta} - a(ae - \ell) \right], \quad (2.27)$$

$$u^r = \pm \frac{1}{r^2} \sqrt{T^2 - \Delta [r^2 + (\ell - ae)^2]}, \quad (2.28)$$

$$u^\varphi = \frac{1}{r^2} \left[\frac{aT}{\Delta} - (ae - \ell) \right], \quad (2.29)$$

where $T \equiv e(r^2 + a^2) - \ell a$.

Let us consider a particle collision of two massive particles, named particles 1 and 2, with equal mass m . For both particle i ($i = 1, 2$), we write u^μ , e , and ℓ as u_i^μ , e_i , and ℓ_i , respectively. We assume that each particle is at rest at infinity, i.e., $e_i = 1$. In this case, the CM energy is given by

$$E_{\text{cm}}^2 = \frac{2m^2}{r\Delta} \left[2a^2(r + M) - 2Ma(\ell_1 + \ell_2) - \ell_2\ell_1(r - 2M) + 2(r - M)r^2 - \sqrt{2M(a - \ell_1)^2 - \ell_1^2 r + 2Mr^2} \sqrt{2M(a - \ell_2)^2 - \ell_2^2 r + 2Mr^2} \right]. \quad (2.30)$$

In the previous subsection, we have seen that the CM energy diverge if either of particles 1 and 2 satisfies the critical condition. However, the critical particle can approach the event horizon only when $a_* = 1$, i.e., the extremal Kerr black hole spacetime. In the extremal case, the CM energy at the horizon r_+ becomes simpler as

$$\lim_{r \rightarrow r_+} E_{\text{cm}} = \sqrt{2}m \sqrt{\frac{\ell_2 - 2M}{\ell_1 - 2M} + \frac{\ell_1 - 2M}{\ell_2 - 2M}}, \quad (2.31)$$

and the critical condition is expressed as $\ell_i - 2M = 0$.

Here we showed that the CM energy can be arbitrarily large, even if the mass and energy of two colliding particles are finite and they are at rest at infinity. This process is so-called the ‘‘BSW process.’’

2.3 Energy extraction process

Since the Killing vector ξ^μ becomes spacelike inside the ergoregion, the conserved energy $E \equiv -\xi^\mu p_\mu$ can be either positive or negative. We note that particles with negative energy can exist only inside of the ergoregion and $E < 0$ means the energy that would be observed at infinity if the particle could be carried there. This existence of the negative energy particle can use the energy extraction from the Kerr black hole.

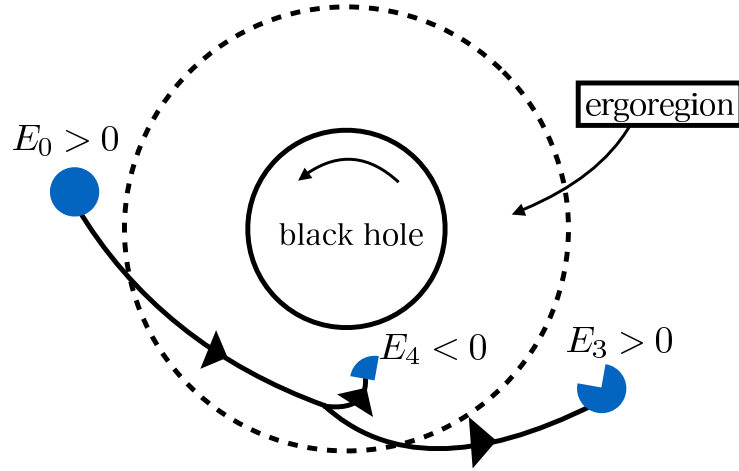


Figure 2.2: The schematic picture of the Penrose process for extracting energy from the Kerr black hole.

2.3.1 Penrose process

In 1969, Penrose [45] pointed out the energy extraction process by using particle division. Let us consider the following situation. A particle with $E_0 > 0$ comes from infinity and it decays into two particles inside the ergoregion. One of the particles falls into a black hole with negative energy $E_4 < 0$ while the other particle escapes to infinity with $E_3 > 0$. See Fig. 2.2. From the conservation of energy $E_0 = E_3 + E_4$, we obtain

$$E_3 = E_0 - E_4 > E_0. \quad (2.32)$$

Because the energy of the escaping particle E_3 is larger than the energy of the initial particle E_0 , the black hole loses own energy, i.e., the energy of the black hole is extracted. This process is so-called ‘‘Penrose process.’’

The Penrose process has an upper limit of the extraction energy because it makes spin-down of the Kerr black hole. As a result, when the spin parameter a becomes zero, the ergoregion is no longer present, and no further the energy extraction occurs. To see this upper limit of the extraction energy in detail, we use the fact that the Killing vector χ^μ , defined by Eq. (2.8), is timelike just outside the event horizon. Hence for any particle, which includes all negative energy particles, the combination $-\chi^\mu p_\mu$ must be positive

$$-\chi^\mu p_\mu = -(\xi^\mu + \Omega_H \psi^\mu) p_\mu = E - \Omega_H L > 0. \quad (2.33)$$

Thus, we obtain

$$L < \frac{E}{\Omega_H}. \quad (2.34)$$

This implies that L must be negative if $E < 0$. Since the negative energy particle carries negative angular momentum to the black hole, the black hole will lose angular momentum during the Penrose process. The angular momentum of the black hole will go to zero, i.e., $a \rightarrow 0$, the ergoregion will disappear, and finally, the Penrose process will stop [59, 60].

The quantitative energy ranges of the decaying particle in the Penrose process is shown in Refs. [61, 62]. We consider a case where the particle with initial energy E and mass m decays into a particle with energy E' and mass m' on the event horizon at the equatorial plane of the extremal Kerr black hole. In this case, we have

$$\gamma \frac{E}{m} - \gamma v \sqrt{\frac{E^2}{m^2} + 1} \leq \frac{E'}{m'} \leq \gamma \frac{E}{m} + \gamma v \sqrt{\frac{E^2}{m^2} + 1}, \quad (2.35)$$

where γ and v are the Lorentz factor and velocity of the decaying particle in the rest frame of the original particle. When the original particle is at rest at infinity ($E/m = 1$) and decays into two particles with m' , the lower energy limit can be negative if $v > 1/\sqrt{2}$. This is equivalent to two decaying particles each with the rest mass of only 35% of the original particle. If the original particle decay into two massless particles, we obtain

$$E' \leq \frac{1 + \sqrt{2}}{2} E \simeq 1.207E. \quad (2.36)$$

This is the upper limit of the energy extraction in the Penrose process.

2.3.2 Collisional and super-Penrose process

A bit modified process of the Penrose process called the collisional Penrose process [2, 46], in which two particles collide in the ergoregion instead of a single particle decay. The maximum energy extraction efficiency can reach about 14 for head-on collisions [49], which is exactly given by $(2 + \sqrt{3})^2$ [50, 51, 52]. More efficient energy extraction is possible by more general head-on collisions, which is called the super-Penrose process [53]. In this thesis, we distinguish between the two processes according to the origin of the colliding particles described below:

Collisional Penrose process: Two colliding particles come from infinity and collide in the ergoregion. We consider both a rear-end collision and a head-on collision. This process is discussed in Chap. 5.

Super-Penrose process: One of the two collision particles is generated in the ergoregion and initially moves outwardly. The trajectory of this particle cannot be realized with particles which came from infinity. In the super-Penrose process, a radially outward particle must be created near the horizon by some preceding process but we will not discuss the details. This process is discussed in Chap. 6.

Chapter 3

High energy particle collision near a BTZ black hole

We consider a particle collision with an arbitrarily large CM energy near a rotating BTZ black hole motivated by further investigations for the effect of the self-gravity on a high energy collision, see Chap. 4. We obtain the CM energy of two general colliding geodesic particles in the BTZ black hole spacetime. We show that the CM energy of two ingoing particles can be arbitrarily large on the event horizon if either of the two particles has a critical angular momentum and the other has a noncritical angular momentum. We also show that a motion of a particle with a subcritical angular momentum is allowed near the extremal BTZ black hole and that the CM energy for a rear-end collision at a point can be arbitrarily large in a critical angular momentum limit.

One may suspect that the negative cosmological constant affects the particle collision, and it is different from the BSW process. However, the effect of the negative cosmological constant on the collision will be negligible since the collision with a high CM energy occurs near an extremal event horizon.

In this chapter, we use the units in which the speed of light and $8G$ are unity as in Sec III in Ref. [34], where G is Newton's constant in three dimensions.

3.1 Particle motion in the BTZ black hole

3.1.1 BTZ spacetime

The line element in the BTZ spacetime [37, 38] is given by

$$ds^2 = -f(r)dt^2 + \frac{dr^2}{f(r)} + r^2 [d\varphi - \Omega(r)dt]^2, \quad (3.1)$$

where

$$f(r) \equiv -M + \frac{r^2}{\ell^2} + \frac{J^2}{4r^2}, \quad (3.2)$$

$$\Omega(r) \equiv -\frac{gt_\varphi}{g_{\varphi\varphi}} = \frac{J}{2r^2}, \quad (3.3)$$

$$\ell \equiv \sqrt{\frac{1}{-\Lambda}}. \quad (3.4)$$

Here M , J , and $\Omega(r)$ are the mass, angular momentum, and angular velocity of the spacetime, respectively, and ℓ ¹ is the scale of a curvature related to the negative cosmological constant $\Lambda < 0$. Without loss of generality, we assume that the angular momentum J is nonnegative. In this thesis, we concentrate on the case where M is positive.

If $J \leq \ell M$ is satisfied, the BTZ spacetime is a black hole spacetime and $f(r)$ vanishes at

$$r = r_\pm \equiv \ell \sqrt{\frac{M}{2} \left(1 \pm \sqrt{1 - \frac{J^2}{\ell^2 M^2}} \right)}, \quad (3.5)$$

where r_+ and r_- correspond to outer and inner horizons, respectively. The BTZ black hole with $J = \ell M$ is known as an extremal black hole and the outer and inner horizons of the extremal BTZ black hole coincide,

$$r_+ = r_- = \ell \sqrt{\frac{M}{2}}. \quad (3.6)$$

If $J > \ell M$ is satisfied, the BTZ spacetime is a naked singularity spacetime and $f(r) = 0$ has no real roots.

Using the horizon radius r_\pm , $f(r)$, $\Omega(r)$, M , and J are expressed as

$$f(r) = \frac{(r^2 - r_+^2)(r^2 - r_-^2)}{\ell^2 r^2}, \quad \Omega(r) = \frac{r_+ r_-}{\ell r^2},$$

$$M = \frac{r_+^2 + r_-^2}{\ell^2}, \quad \text{and} \quad J = \frac{2r_+ r_-}{\ell}, \quad (3.7)$$

respectively.

3.1.2 General geodesic of a particle

The BTZ spacetime is stationary and axisymmetric with corresponding two Killing vectors ξ^μ and ψ^μ , where $\xi^\mu \partial_\mu = \partial_t$ and $\psi^\mu \partial_\mu = \partial_\varphi$. The conserved energy E and angular momentum L of a particle with 3-momentum p^μ are defined as

$$E \equiv -g_{\mu\nu} \xi^\mu p^\nu, \quad (3.8)$$

¹ In this chapter, ℓ denote the scale of a curvature rather than a specific angular momentum.

and

$$L \equiv g_{\mu\nu}\psi^\mu p^\nu, \quad (3.9)$$

respectively. These two conserved quantities are constant along a geodesic for the particle.

From the normalization condition of the 3-momentum $p^\mu p_\mu = -m^2$ and Eqs. (3.8) and (3.9), the components of the 3-momentum are given by

$$p^t = \frac{S(r)}{f(r)}, \quad (3.10)$$

$$p^r = \sigma\sqrt{R(r)}, \quad (3.11)$$

$$p^\varphi = \frac{\Omega(r)S(r)}{f(r)} + \frac{L}{r^2}, \quad (3.12)$$

where $\sigma \equiv \text{sgn}(p^r)$,

$$S(r) \equiv E - \Omega(r)L, \quad (3.13)$$

$$R(r) \equiv S^2(r) - \left(m^2 + \frac{L^2}{r^2}\right)f(r), \quad (3.14)$$

and m denotes a rest mass of the particle.

We assume the forward-in-time condition $p^t \geq 0$ for the particle motion. This condition implies that the coordinate t increases along the particle motion.

We call a condition $S(r_+) = 0$ a critical condition. The critical condition is rewritten as

$$E - \Omega_H L = 0, \quad (3.15)$$

where

$$\Omega_H \equiv \Omega(r_+) = \frac{J}{2r_+^2} = \frac{r_-}{\ell r_+}, \quad (3.16)$$

is the angular velocity of the horizon. We define a critical angular momentum L_c as

$$L_c \equiv \frac{\ell r_+}{r_-} E. \quad (3.17)$$

We call a particle a critical particle if it has the critical angular momentum, for which satisfies Eq. (3.15). Accordingly, we call a particle with $L < L_c$ ($L > L_c$) a subcritical (supercritical) particle.

The particle motion is restricted to a region where $R(r)$ is nonnegative. The particle can exist at the event horizon because of $R(r_+) = S^2(r_+) \geq 0$. If particle has a mass, it cannot exist at infinity because

$$\lim_{r \rightarrow \infty} R(r) = \lim_{r \rightarrow \infty} -\frac{m^2 r^2}{\ell^2} < 0. \quad (3.18)$$

For a massless particle, $R(r)$ is expressed as

$$R(r) = E^2 - \frac{L^2}{\ell^2} + \frac{L}{\ell r^2} \left[-2Er_+r_- + \frac{L}{\ell}(r_+^2 + r_-^2) \right] \quad (3.19)$$

If $-E\ell \leq L \leq E\ell$ is satisfied, $R(r)$ is nonnegative in the region $r_+ \leq r$. On the other hand, if $L < -E\ell$ or $E\ell < L$ is satisfied, $R(r)$ is nonnegative in the region $r_+ \leq r \leq r_0$, where

$$r_0 \equiv r_+ \sqrt{1 - \frac{\ell S^2(r_+)}{E^2 \ell^2 - L^2}} > r_+. \quad (3.20)$$

3.1.3 Motion of a critical particle

We investigate the motion of a particle with the critical angular momentum L_c . Substituting Eq. (3.17) into Eqs. (3.10), (3.11), and (3.12), we obtain the components of the 3-momentum of the critical particle as

$$p^t = \frac{E\ell^2}{r^2 - r_-^2}, \quad (3.21)$$

$$p^r = \sigma \sqrt{R(r)}, \quad (3.22)$$

$$p^\varphi = \frac{E\ell r_+}{(r^2 - r_-^2)r_-}, \quad (3.23)$$

where

$$R(r) = R_c(r) \equiv -\frac{r^2 - r_+^2}{r^2} \left[\frac{E^2(r_+^2 - r_-^2)}{r_-^2} + \frac{m^2(r^2 - r_-^2)}{\ell^2} \right]. \quad (3.24)$$

The above expression shows $R_c(r_+) = 0$ and $R_c(r) < 0$ in the region $r_+ < r$. Therefore, the critical particle cannot exist outside of the event horizon $r_+ < r$. The derivative of $R_c(r)$ with respect to r is given by

$$R'_c(r) = -\frac{2m^2 r}{\ell^2} + \frac{2r_+^2 [-E^2 \ell^2 (r_+^2 - r_-^2) + r_-^4 m^2]}{\ell^2 r_-^2 r^3}, \quad (3.25)$$

where a prime denotes a derivative with respect to r and it becomes

$$R'_c(r_+) = -\frac{2(r_+^2 - r_-^2)(E^2 \ell^2 + r_-^2 m^2)}{\ell^2 r_+ r_-^2} \leq 0, \quad (3.26)$$

on the event horizon.

In the extremal case, i.e., $r_+ = r_-$, we obtain

$$R_c(r) = -\frac{m^2(r^2 - r_+^2)^2}{\ell^2 r^2}, \quad (3.27)$$

$$R'_c(r) = -\frac{2m^2(r^2 + r_+^2)(r^2 - r_+^2)}{\ell^2 r^3}. \quad (3.28)$$

Therefore, we obtain $R_c(r_+) = R'_c(r_+) = 0$ on the event horizon.

3.1.4 Motion of a subcritical particle

We consider the motion of a particle with the subcritical angular momentum

$$L = L_c - \frac{\ell r_+}{r_-} \delta = \frac{\ell r_+ (E - \delta)}{r_-}, \quad (3.29)$$

where δ is a positive constant. From Eq. (3.14), $R(r)$ is expressed as

$$R(r) = R_c(r) + \frac{r_+^2 \delta [2E(r^2 - r_+^2) - (r^2 - r_+^2 - r_-^2) \delta]}{r_-^2 r^2}. \quad (3.30)$$

The particle with the subcritical angular momentum can exist on the event horizon and near the black hole since

$$R(r_+) = \delta^2 > 0. \quad (3.31)$$

The derivative of $R(r)$ with respect r is given by

$$R'(r) = R'_c(r) + \frac{2r_+^2 \delta [2Er_+^2 - (r_+^2 + r_-^2) \delta]}{r_-^2 r^3}, \quad (3.32)$$

and it becomes

$$R'(r_+) = R'_c(r_+) + \frac{2\delta [2Er_+^2 - (r_+^2 + r_-^2) \delta]}{r_+ r_-^2} \quad (3.33)$$

on the event horizon.

From Eqs. (3.26) and (3.33), $R'_c(r)$ is a quadratic equation with respect to δ . After some straightforward calculation, we obtain the following results. When $E < E_m$, $R'_c(r)$ is negative, where

$$E_m \equiv \frac{m \sqrt{r_+^4 - r_-^4}}{\ell r_-}. \quad (3.34)$$

When $E \geq E_m$, $R'_c(r)$ is nonnegative if and only if $\delta_L \leq \delta \leq \delta_R$ is satisfied. Here δ_L and δ_R are defined as

$$\delta_L \equiv \frac{E \ell r_+^2 - r_- \sqrt{E^2 \ell^2 r_-^2 - (r_+^4 - r_-^4) m^2}}{\ell (r_+^2 + r_-^2)}, \quad (3.35)$$

and

$$\delta_R \equiv \frac{E \ell r_+^2 + r_- \sqrt{E^2 \ell^2 r_-^2 - (r_+^4 - r_-^4) m^2}}{\ell (r_+^2 + r_-^2)}, \quad (3.36)$$

respectively. We note that an inequality $0 \leq \delta_L \leq \delta_R \leq E$ is satisfied by definitions.

If $E \geq E_m$ and $\delta_L \leq \delta \leq \delta_R$ are satisfied, $R'(r) = 0$ has only two real solutions. Either of the two solutions is positive and the other solution is negative. The positive solution is given by

$$r = r_m \equiv \left(1 + \frac{\ell^2 R'(r_+)}{2r_+ m^2}\right)^{\frac{1}{4}} r_+ \geq r_+. \quad (3.37)$$

As r increases from r_+ to infinity, $R(r)$ begins with $R(r_+) = \delta^2$, monotonically increases to a local maximum $R(r_m) > \delta^2$ at $r = r_m$, and monotonically decreases to negative infinity.

In the extremal BTZ black hole case, i.e., $r_+ = r_-$, we obtain

$$E_m = 0, \quad \delta_L = 0, \quad \text{and} \quad \delta_R = E, \quad (3.38)$$

furthermore

$$r_m \rightarrow r_+, \quad R(r_+) \rightarrow 0, \quad \text{and} \quad R'(r_+) \rightarrow 0, \quad (3.39)$$

in the critical angular momentum limit $\delta \rightarrow 0$.

3.2 CM energy for particle collisions

We consider a collision of two particles, named particles 1 and 2, in the BTZ spacetime. For both particles i ($i=1,2$), we write p^μ , m , E , L , and σ as p_i^μ , m_i , E_i , L_i , and σ_i , respectively. From Eq. (2.19), the CM energy of the two particles is given by

$$E_{\text{cm}}^2(r) = m_1^2 + m_2^2 + 2 \frac{S_1(r)S_2(r) - \sigma_1\sigma_2\sqrt{R_1(r)R_2(r)}}{f(r)} - \frac{2L_1L_2}{r^2}, \quad (3.40)$$

where $S_i(r)$ and $R_i(r)$ are defined as

$$S_i(r) \equiv E_i - \frac{r_+ r_-}{\ell r^2} L_i \quad \text{and} \quad R_i(r) \equiv S_i^2(r) - \left(m_i^2 + \frac{L_i^2}{r^2}\right) f(r), \quad (3.41)$$

respectively.

3.2.1 General colliding particles

We consider a rear-end collision of two ingoing particles, i.e., we choose $\sigma_1 = \sigma_2 = -1$. Since both the numerator and denominator of the third term in Eq. (3.40) vanish at the horizon, we use l'Hopital's rule to estimate it and we obtain

$$\lim_{r \rightarrow r_+} 2 \frac{S_1(r)S_2(r) - \sqrt{R_1(r)R_2(r)}}{f(r)} = \frac{S_2(r_+)}{S_1(r_+)} \left(\frac{L_1^2}{r_+^2} + m_1^2\right) + \frac{S_1(r_+)}{S_2(r_+)} \left(\frac{L_2^2}{r_+^2} + m_2^2\right). \quad (3.42)$$

Therefore, the CM energy in the near horizon $r \rightarrow r_+$ is obtained as

$$\lim_{r \rightarrow r_+} E_{\text{cm}}^2(r) = m_1^2 + m_2^2 + \frac{S_2(r_+)}{S_1(r_+)} \left(\frac{L_1^2}{r_+^2} + m_1^2 \right) + \frac{S_1(r_+)}{S_2(r_+)} \left(\frac{L_2^2}{r_+^2} + m_2^2 \right) - \frac{2L_1L_2}{r_+^2}. \quad (3.43)$$

This show that the CM energy of the rear-end collision can be arbitrarily large if and only if either of the colliding particles satisfies the critical condition. When both the particles satisfy the critical condition, the CM energy in the near horizon $r \rightarrow r_+$ becomes finite as

$$\lim_{r \rightarrow r_+} E_{\text{cm}}^2(r) = \left(1 + \frac{E_2}{E_1} \right) m_1^2 + \left(1 + \frac{E_1}{E_2} \right) m_2^2. \quad (3.44)$$

3.2.2 Critical angular momentum limit

Next, we consider a rear-end collision of two ingoing particles in the extremal BTZ black hole. We assume that particle 1 has a subcritical angular momentum

$$L_1 = \ell(E_1 - \delta) \leq L_{c1}, \quad (3.45)$$

where δ satisfies $0 = \delta_{L1} \leq \delta \leq \delta_{R1} = E_1$, and particle 2 has a subcritical angular momentum $L_2 < L_{c2}$. We consider a particle collision at $r = r_m$ where

$$r_m = \left(1 + \frac{\ell^2 R_1'(r_+)}{2r_+ m_1^2} \right)^{\frac{1}{4}} r_+ \geq r_+. \quad (3.46)$$

Here, δ_{L1} , δ_{R1} , and $R_1'(r)$ are δ_L , δ_R , and $R'(r)$ for particle 1, respectively, and L_{ci} is the the critical angular momentum for particle i .

From Eq. (3.40), the CM energy of the rear-end collision at $r = r_m$ in the critical angular momentum limit $\delta \rightarrow 0$ is given by

$$\lim_{\delta \rightarrow 0} E_{\text{cm}}^2(r_m) = m_1^2 + m_2^2 + 2\Gamma - \frac{2E_1L_2\ell}{r_+^2}, \quad (3.47)$$

where Γ is defined as

$$\Gamma \equiv \lim_{\delta \rightarrow 0} \frac{S_1(r_m)S_2(r_m) - \sqrt{R_1(r_m)R_2(r_m)}}{f(r_m)}. \quad (3.48)$$

Both the numerator and denominator of Γ vanish in the critical angular momentum limit. Using l'Hopital's rule with respect to δ , Γ is expressed as

$$\Gamma = \lim_{\delta \rightarrow 0} \frac{S_2(r_m)}{\dot{f}(r_m)} \left(\dot{S}_1(r_m) - \frac{\dot{R}_1(r_m)}{2\sqrt{R_1(r_m)}} \right), \quad (3.49)$$

where a dot denotes a derivative with respect to δ . Since both the numerator and denominator of the second term in the above equation vanish, we use l'Hopital's

rule again to estimate it and we obtain, after a straightforward calculation,

$$\lim_{\delta \rightarrow 0} \frac{\dot{R}_1(r_m)}{2\sqrt{R_1(r_m)}} = \lim_{\delta \rightarrow 0} \sqrt{\frac{\ddot{R}_1(r_m)}{2}} = \lim_{\delta \rightarrow 0} \sqrt{\dot{S}_1(r_m)}, \quad (3.50)$$

where

$$\lim_{\delta \rightarrow 0} \dot{S}_1(r_m) = 1 + \frac{E_1^2 \ell^2}{r_+^2 m_2^2}. \quad (3.51)$$

Thus, Γ is obtained as

$$\Gamma = \lim_{\delta \rightarrow 0} \frac{S_2(r_m) \left(\dot{S}_1(r_m) - \sqrt{\dot{S}_1(r_m)} \right) r_+^2 m_1^4}{E_1^2 \ell^2 \delta} \rightarrow \infty. \quad (3.52)$$

Therefore, the CM energy $E_{\text{cm}}(r_m)$ of the rear-end collision at the point $r = r_m$ diverges in the critical angular momentum limit $\delta \rightarrow 0$.

Chapter 4

Collision of two thin shells in the BTZ spacetime

We consider a collision of two dust thin shells with a high CM energy including their self-gravity in a rotating BTZ spacetime. The shells divide the BTZ spacetime into three domains and the domains are matched by the Darmois-Israel junction conditions. We treat only the collision of two shells which corotate with a background BTZ spacetime because of the junction conditions. The counterpart of the corotating shell collision is a collision of two particles with vanishing angular momenta. We compare the dust thin shell collision and the particle collision in order to investigate the effects of the self-gravity of colliding objects on the high CM energy collision. We show that the self-gravity of the shells affects the position of an event horizon and it covers the high-energy collisional event. Therefore, we conclude that the self-gravity of colliding objects suppresses its CM energy and that any observer who stands outside of the event horizon cannot observe the collision with an arbitrary high CM energy.

In this chapter, r^H denote the horizon radius instead of r_+ and we use the units in which the speed of light and $8G$ are unity as in Sec III in Ref. [34], where G is Newton's constant in three dimensions.

4.1 Collision of two particles with vanishing angular momenta

First, we consider a collision of two particles with vanishing angular momenta as the counterpart of the shell collision.

The angular velocity of a particle $\omega(r)$ is defined as

$$\omega(r) \equiv \frac{d\varphi}{dt} = \frac{p^\varphi}{p^t}. \quad (4.1)$$

When a particle has a zero conserved angular momentum $L = 0$, from Eqs. (3.10), (3.12), and (4.1), the angular velocity of the particle coincides with the angular velocity of the spacetime, i.e., $\omega(r) = \Omega(r)$. This means that the particle with $L = 0$ corotates with the background spacetime.

From Eq. (3.11), the energy equation which describes the radial motion of the particle is given by

$$\left(\frac{dr}{d\tau}\right)^2 + V(r) = 0, \quad (4.2)$$

where $V(r)$ is the effective potential for the radial motion of the particle and τ is its proper time. Here we have used relations $p^\mu = mu^\mu$ and $u^\mu = dx^\mu/d\tau$, where m and u^μ are the rest mass and 3-velocity, respectively. The particle motion is restricted to the region where $V(r) \leq 0$. Using a dimensionless radial coordinate $x \equiv r/\ell$, the effective potential with the specific energy $e \equiv E/m$ and the position of the event horizon are expressed as

$$V(x) = -e^2 + f(x) = x^2 - M - e^2 + \frac{j^2}{4x^2}, \quad (4.3)$$

and

$$x^H \equiv \frac{r^H}{\ell} = \sqrt{\frac{M + \sqrt{M^2 - j^2}}{2}}, \quad (4.4)$$

respectively, where

$$f(x) = x^2 - M + \frac{j^2}{4x^2}, \quad j \equiv \frac{J}{\ell}. \quad (4.5)$$

As x increases from 0 to infinity, $V(x)$ and $f(x)$ begin with infinity, monotonically decrease to a local minimum at $x = x^m \equiv \sqrt{j/2}$, and monotonically increase to infinity. The positive solutions of $V(x) = 0$ are given by

$$x = x^\pm \equiv \sqrt{\frac{M + e^2 \pm \sqrt{(M + e^2)^2 - j^2}}{2}}. \quad (4.6)$$

Therefore, a motion of the particle is restricted to the region $x^- \leq x \leq x^+$. We notice that a relation

$$x^- \leq x^m \leq x^H \leq x^+, \quad (4.7)$$

is satisfied and we obtain $x^m = x^H$ ($x^H = x^+$) in the extremal (critical) case and $x^- = x^m = x^H = x^+$ in the extremal and critical case.

We consider a collision of two particles, named particle 1 and 2, with vanishing conserved angular momenta $L_1 = L_2 = 0$. For both particle i ($i = 1, 2$),

we write e , L , m , σ , $V(r)$, and x^\pm as e_i , L_i , m_i , σ_i , $V_i(r)$, and x_i^\pm , respectively. The CM energy $E_{\text{cm}}(x)$ of the particles is given by

$$E_{\text{cm}}^2(x) = m_1^2 + m_2^2 + 2m_1m_2 \frac{e_1e_2 - \sigma_1\sigma_2\sqrt{V_1(x)V_2(x)}}{f(x)}. \quad (4.8)$$

We consider a rear-end collision, i.e., $\sigma_1 = \sigma_2 = -1$, and assume that a collision occur in a region $x^H \leq x \leq x_i^+$ where is seen by an observer who stands at the outside of the horizon x^H .

In this case, as x increases from x^H to x_i^+ , the CM energy begins with

$$E_{\text{cm}}(x^H) = \sqrt{m_1^2 + m_2^2 + m_1m_2 \left(\frac{e_2}{e_1} + \frac{e_1}{e_2} \right)}, \quad (4.9)$$

and monotonically increases to

$$E_{\text{cm}}(x_i^+) = \sqrt{m_1^2 + m_2^2 + 2m_1m_2 \frac{e_1e_2}{e_i^2}}. \quad (4.10)$$

Here we have used l'Hopital's rule to estimate $E_{\text{cm}}(x^H)$. We get $E_{\text{cm}}(x) = m_1 + m_2$ if the both particles have a same specific energy $e_1 = e_2$.

From Eq. (3.15), the critical condition for particle i ($i = 1, 2$) with $L_i = 0$ is given by

$$E_i = 0, \text{ i.e., } e_i = 0. \quad (4.11)$$

We are interested in the collision of the inner particle 1 with a critical limit $e_1 \rightarrow 0$ and the outer particle 2 which is not critical in the extremal BTZ spacetime since the collision will correspond with the BSW collision in the extremal Kerr spacetime [1] and in the extremal Reissner-Nordström spacetime [27]. In this case, the collisional point must be $x \rightarrow x^H + 0$ because of inequality (4.7) and $x_1^\pm \rightarrow x^H \pm 0$ and the CM energy E_{cm} diverges there.

We note that a critical particle has $V_1(x^H) = V_1'(x^H) = 0$ and $V_1''(x^H) > 0$, where a prime denotes a derivative with respect to x , in the extremal BTZ spacetime while one has $V_1(x^H) = V_1'(x^H) = 0$ and $V_1''(x^H) < 0$ in an extremal Kerr black hole spacetime and an extremal Reissner-Nordström spacetime. The positive sign of $V_1''(x^H)$ is caused by the negative cosmological constant and it will not affect on the BSW collision strongly since the collision happens on the horizon.

4.2 Thin shell and its motion in the BTZ spacetime

In this section, as a preparation to study a shell collision, we review the Darmois-Israel junction conditions [60, 63, 64] and a motion of a dust thin shell in the BTZ spacetime [34].

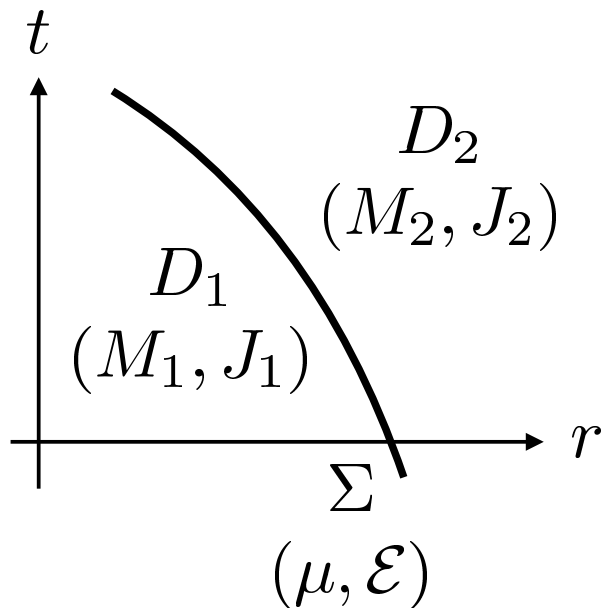


Figure 4.1: The schematic picture of the BTZ spacetime divided into two domains D_1 and D_2 by the hypersurface Σ . Both domains D_A ($A = 1, 2$) are the BTZ spacetime with the same scale of the curvature ℓ , but different masses M_A and angular momenta J_A . A thin shell on the hypersurface Σ has a proper mass μ and specific energy $\mathcal{E} \equiv (M_2 - M_1)/\mu$.

We consider a two-dimensional hypersurface Σ which divides the BTZ spacetime into an interior domain D_1 and an exterior domain D_2 . For simplicity, we assume that both domains D_A ($A = 1, 2$) are the BTZ spacetime with the same scale of the curvature ℓ , but different masses M_A and angular momenta J_A , where M_A and J_A are M and J for D_A , respectively. See Fig. 4.1 for the schematic picture of the BTZ spacetime divided into two domains D_1 and D_2 by the hypersurface Σ . Hereinafter, we use x^μ denoting coordinates in every domain and y^i denoting same coordinates in both the side of Σ for simplicity.

The projection operator from the ambient spacetime to Σ is defined as

$$e_{Ai}^\mu \equiv \frac{\partial x_A^\mu}{\partial y^i}. \quad (4.12)$$

The induced metric on Σ and the extrinsic curvature are defined as

$$h_{ij} \equiv g_{\mu\nu}^A e_{Ai}^\mu e_{Aj}^\nu, \quad (4.13)$$

and

$$K_{ij}^A \equiv e_{Ai}^\mu e_{Aj}^\nu \nabla_\mu^A n_\nu, \quad (4.14)$$

respectively, where ∇_μ^A is the covariant derivative within D_A and n_μ is the unit normal vector, which is directed from D_1 to D_2 . The first and second junction conditions are given by

$$[h_{ij}] = 0 \quad \text{and} \quad [K_{ij}] = 0, \quad (4.15)$$

respectively. Here, the bracket is defined as

$$[\Psi] \equiv \Psi(D_2)|_\Sigma - \Psi(D_1)|_\Sigma, \quad (4.16)$$

where Ψ is any quantity defined on the both sides of Σ .

We assume that the thin shell is at $r = \mathcal{R}(t)$ since we are interested in a motion of the shell on Σ . It is useful to convert to a frame that is comoving with the shell, i.e., a corotating frame, by making the following change of azimuth coordinates

$$d\varphi \rightarrow d\phi + \frac{J_A}{2\mathcal{R}^2(t)} dt. \quad (4.17)$$

The metric in D_A then becomes

$$\begin{aligned} ds_A^2 &= g_{\mu\nu}^A dx^\mu dx^\nu \\ &= -f_A(r) dt^2 + \frac{dr^2}{f_A(r)} + r^2 \left[d\phi + \frac{J_A}{2} \left(\frac{1}{\mathcal{R}^2(t)} - \frac{1}{r^2} \right) dt \right]^2, \end{aligned} \quad (4.18)$$

where

$$f_A(r) \equiv -M_A + \frac{r^2}{\ell^2} + \frac{J_A^2}{4r^2}. \quad (4.19)$$

The trajectory of the shell is parametrized by the proper time τ as

$$t = \mathcal{T}(\tau) \quad \text{and} \quad r = \mathcal{R}(\mathcal{T}(\tau)) = \mathcal{R}(\tau). \quad (4.20)$$

From the first junction condition $[h_{ij}] = 0$, the induced metric h_{ij} on Σ is given by

$$\begin{aligned} ds_\Sigma^2 &= h_{ij} dx^i dx^j = -d\tau^2 + \mathcal{R}^2(\tau) d\phi^2 \\ &= \left[-f_A(\mathcal{R}) \dot{\mathcal{T}}^2 + \frac{\dot{\mathcal{R}}^2}{f_A(\mathcal{R})} \right] d\tau^2 + \mathcal{R}^2(\tau) d\phi^2, \end{aligned} \quad (4.21)$$

where a dot denotes a derivative with respect to τ . This implies

$$f_A(\mathcal{R}) \dot{\mathcal{T}} = \sqrt{\dot{\mathcal{R}}^2 + f_A(\mathcal{R})} \equiv \beta_A. \quad (4.22)$$

The induced basis vectors e_i^μ and the unit normal vector n_μ to Σ are given by

$$e_\tau^\mu = (\dot{\mathcal{T}}, \dot{\mathcal{R}}, 0), \quad e_\phi^\mu = (0, 0, 1), \quad (4.23)$$

and

$$n_\mu = (-\dot{\mathcal{R}}, \dot{\mathcal{T}}, 0), \quad (4.24)$$

respectively. Substituting the above expressions into Eq. (4.14), we obtain the components of the extrinsic curvature and its trace $K^A \equiv h^{ij} K_{ij}^A$ as

$$K_{\tau\tau}^A = -\frac{\dot{\beta}_A}{\mathcal{R}}, \quad K_{\phi\phi}^A = \mathcal{R}\beta_A, \quad K_{\tau\phi}^A = \frac{J_A}{2\mathcal{R}}, \quad (4.25)$$

and

$$K^A = \frac{\dot{\beta}_A}{\mathcal{R}} + \frac{\beta_A}{\mathcal{R}}, \quad (4.26)$$

respectively. We note that the second junction condition $[K_{ij}] = 0$ is violated unless we consider a trivial case. Therefore we introduce a thin shell on Σ following equations

$$\pi S_{ij} = -([K_{ij}] - h_{ij}[K]), \quad (4.27)$$

where S_{ij} is the surface stress-energy tensor of the thin shell. We assume that the thin shell is a dust thin shell, i.e., the surface stress-energy tensor S_{ij} is given by

$$S_{ij} = \rho u_i u_j, \quad (4.28)$$

where ρ and $u_i = (-1, 0)$ are the surface energy density and the 2-velocity of the shell, respectively.

By using Eqs. (4.25), (4.26), and (4.28), we write down Eq. (4.27) and obtain

$$[\beta] + \pi\rho\mathcal{R} = 0, \quad (4.29)$$

$$[\dot{\beta}] = 0, \quad (4.30)$$

$$[J] = 0. \quad (4.31)$$

From Eqs. (4.29) and (4.30), we obtain

$$\frac{d}{d\tau}(\pi\rho\mathcal{R}) = 0. \quad (4.32)$$

Therefore, we can define a constant μ as

$$\mu \equiv 2\pi\rho\mathcal{R}. \quad (4.33)$$

This constant μ is interpreted as the proper mass of the shell and it is conserved along a trajectory. We define the specific energy \mathcal{E} of the shell as

$$\mathcal{E} \equiv \frac{[M]}{\mu} = \frac{M_2 - M_1}{\mu}. \quad (4.34)$$

We assume that the proper mass μ and specific energy \mathcal{E} are positive. This implies that the masses satisfy the relation $M_1 < M_2$. From Eq. (4.31), the deviation of the angular momentum must be zero, i.e.,

$$J \equiv J_1 = J_2. \quad (4.35)$$

Employing expression Eq. (4.22), we obtain an equation for the radial motion of the shell as

$$\left(\frac{d\mathcal{R}}{d\tau}\right)^2 + V(\mathcal{R}) = 0, \quad (4.36)$$

where $V(\mathcal{R})$ is the effective potential of the shell motion. When we define the dimensionless parameter $x \equiv \mathcal{R}/\ell$, the effective potential is expressed as

$$V(x) = -Z^2 + f(x) = x^2 - \left(\frac{\mu^2}{16} + \frac{M_2 + M_1}{2} + \mathcal{E}^2\right) + \frac{j^2}{4x^2}, \quad (4.37)$$

where

$$Z \equiv \frac{\mu}{4} - \mathcal{E}, \quad f(x) \equiv x^2 - M_2 + \frac{j^2}{4x^2}. \quad (4.38)$$

As x increases from 0 to infinity, $V(x)$ and $f(x)$ begin with infinity, monotonically decrease to a local minimum at $x = x^m \equiv \sqrt{j/2}$, and monotonically increase to infinity. The positive solutions of $V(x) = 0$ are given by

$$x = x^\pm \equiv \sqrt{\frac{B \pm \sqrt{B^2 - j^2}}{2}}, \quad (4.39)$$

where

$$B \equiv Z^2 + M_2 = \frac{\mu^2}{16} + \frac{M_2 + M_1}{2} + \mathcal{E}^2. \quad (4.40)$$

Therefore, the shell motion is restricted to the region $x^- \leq x \leq x^+$.

Here we compare the effective potential of a thin shell and particle since the counterpart of the corotating shell motion is a motion of a particle with vanishing angular momentum. From Eqs. (4.3) and (4.37), the effective potential of the particle $V_P(x)$ and shell $V_S(x)$ are given by

$$V_P(x) = x^2 - M - e^2 + \frac{j^2}{4x^2}, \quad (4.41)$$

and

$$V_S(x) = x^2 - \left(\frac{\mu^2}{16} + \frac{M_2 + M_1}{2} + \mathcal{E}^2\right) + \frac{j^2}{4x^2}. \quad (4.42)$$

By comparing the above expressions, we can see that the differences between $V_S(x)$ and $V_P(x)$ are regarded as the self-gravity interaction terms.

If we take limits $\mu \rightarrow 0$ and $M_1 \rightarrow \mathcal{M} \equiv M_2$ with $\mathcal{E} = (\text{const}) \neq 0$, $V_S(x)$ become

$$V_S(x) \rightarrow x^2 - \mathcal{M} - \mathcal{E}^2 + \frac{j^2}{4x^2}. \quad (4.43)$$

Since we can see that the above expression has almost the same as the effective potential of the particle, we may call these limits a test shell limit.

4.3 Collision of two dust thin shells

Here we investigate a collision of two dust thin shells in the BTZ spacetime. We assume that shell 1 and shell 2 are on an inner hypersurface Σ_1 and an outer hypersurface Σ_2 , respectively. These two hypersurfaces divide the BTZ spacetime into an interior domain D_1 , a middle domain D_2 , and an exterior domain D_3 . We assume that all domains D_A ($A = 1, 2, 3$) are the BTZ spacetime with same ℓ , but different masses M_A , where M_A are masses in D_A . From the junction condition Eq. (4.31), all the domains have the same $j \equiv J/\ell$, see Fig. 4.2. As in the Sec. 4.2, we assume $M_1 < M_2 < M_3$ below. We consider five cases according to the value of j as shown in Table 4.1: case I (II) for $j < M_1$ ($j = M_1$), case III for $j = M_2$, and case IV (V) for $j = M_3$ ($j > M_3$).

case	D_1	D_2	D_3	$j \equiv J/\ell$	$X \equiv f(x^m)$
I	S	S	S	$j < M_1$	$X < 0$
II	E	S	S	$j = M_1$	$X < 0$
III	O	E	S	$j = M_2$	$X = 0$
IV	O	O	E	$j = M_3$	$X > 0$
V	O	O	O	$j > M_3$	$X > 0$

Table 4.1: Five cases of the spacetime according to the value of $j \equiv J/\ell$. Symbols S, E, and O denote the sub-extremal, extremal, and over-spinning spacetime, respectively. X is defined as the minimum of $f_2(x)$.

When $j < M_A$ is satisfied, an observer in D_A seems to have the event horizon at $x = x_A^H$, where

$$x_A^H = \sqrt{\frac{M_A + \sqrt{M_A^2 - j^2}}{2}}. \quad (4.44)$$

We note that a position of x_A^H is not always in D_A . It depends on where shells are located.

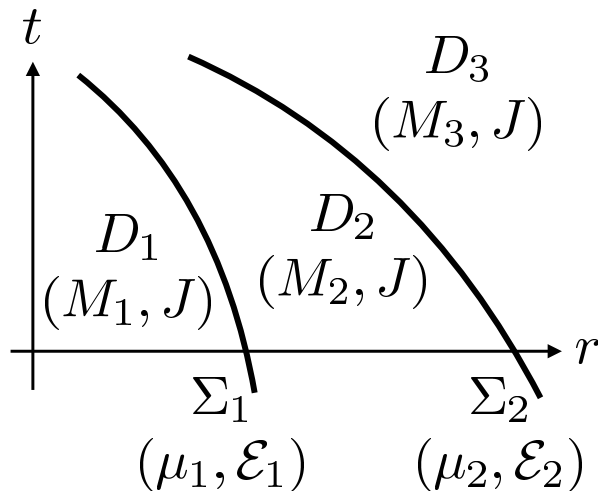


Figure 4.2: The schematic picture of the BTZ spacetime divided into three domains D_1 , D_2 , and D_3 by the two hypersurfaces Σ_1 and Σ_2 . All domains D_A ($A = 1, 2, 3$) are the BTZ spacetime with different masses M_A but the same angular momentum J . A thin shell a ($a = 1, 2$) on the hypersurfaces Σ_a has a proper mass μ_a and specific energy $\mathcal{E}_a \equiv (M_{a+1} - M_a)/\mu_a$.

The effective potential of shell a ($a = 1, 2$) is given by

$$V_a(x) = -Z_a^2 + f(x), \quad (4.45)$$

where

$$Z_1 \equiv \frac{\mu_1}{4} - \mathcal{E}_1, \quad Z_2 \equiv \frac{\mu_2}{2} + \mathcal{E}_2, \quad (4.46)$$

$$f(x) \equiv f_2(x) = x^2 - M_2 + \frac{j^2}{4x^2}. \quad (4.47)$$

Here μ_a and \mathcal{E}_a are the proper mass and specific energy for shell a , respectively.

As x increases from 0 to infinity, $V_a(x)$ begins with infinity, monotonically decreases to a local minimum

$$V_a(x^m) = -Z_a^2 + X, \quad (4.48)$$

where

$$X \equiv f(x^m) = j - M_2, \quad (4.49)$$

at $x = x^m \equiv \sqrt{j/2}$, and monotonically increase to infinity. We note that x^m for shell 1 and 2 are the same.

A motion of shell a is restricted to the region where the effective potential $V_a(x)$ is nonpositive. In order for such the region to exist, the condition

$$X \leq Z_a^2, \quad (4.50)$$

should be satisfied. If the above condition is satisfied, $V_a(x) = 0$ has two positive solutions $x = x_a^\pm$, where

$$x = x_a^\pm \equiv \sqrt{\frac{B_a \pm \sqrt{B_a^2 - j^2}}{2}}, \quad (4.51)$$

and

$$B_a \equiv Z_a^2 + M_2. \quad (4.52)$$

Therefore, the motion of shell a is restricted to the region $x_a^- \leq x \leq x_a^+$.

In Sec. 4.1, we have seen that the critical particle is important in order to realize a particle collision with high CM energy. In this sense, we consider a critical condition for a shell. We can easily show that

$$V_1(x_2^H) = V_1'(x_2^H) = 0, \quad (4.53)$$

is satisfied if and only if $Z_1 = 0$ and $j = M_2$ are satisfied. Therefore, we call a condition

$$Z_1 = 0, \quad (4.54)$$

a critical condition for shell 1.

4.3.1 CM energy

The CM energy $E_{\text{cm}}(x)$ of two shells is given by [29]

$$\begin{aligned} E_{\text{cm}}^2(x) &\equiv -g_{\mu\nu} (\mu_1 U_1^\mu + \mu_2 U_2^\mu) (\mu_1 U_1^\nu + \mu_2 U_2^\nu) \\ &= \mu_1^2 + \mu_2^2 + 2\mu_1\mu_2 \left(\dot{\mathcal{T}}_1 \dot{\mathcal{T}}_2 f(x) - \frac{\dot{\mathcal{R}}_1 \dot{\mathcal{R}}_2}{f(x)} \right), \end{aligned} \quad (4.55)$$

where $g_{\mu\nu}$ is the metric in D_2 ,

$$U_a^\mu = \left(\dot{\mathcal{T}}_a, \dot{\mathcal{R}}_a, 0 \right) = \left(\frac{|Z_a|}{f(x)}, \sigma_a \sqrt{-V_a(x)}, 0 \right), \quad (4.56)$$

is the 3-velocity of the shell a , and $\sigma_a \equiv \text{sgn}(\dot{\mathcal{R}}_a) = \pm 1$.

We concentrate on a rear-end collision of two dust thin shells. In this case, we should choose $\sigma_1 = \sigma_2 = -1$ and the CM energy is expressed as

$$E_{\text{cm}}^2(x) = \mu_1^2 + \mu_2^2 + 2\mu_1\mu_2 \frac{|Z_1|Z_2 - \sqrt{V_1(x)V_2(x)}}{f(x)}, \quad (4.57)$$

We note that if $|Z_1| = Z_2$ is satisfied, the CM energy becomes the total mass of the two shells and it is constant with respect to x , i.e., $E_{\text{cm}}(x) = \mu_1 + \mu_2$.

In order for shell 2 to catch up with shell 1, $\mathcal{R}_2^2 - \mathcal{R}_1^2 \geq 0$, i.e., $V_1(x) \geq V_2(x)$, should be satisfied at a collision point. From the above condition, we obtain

$$Z_1^2 \leq Z_2^2 \text{ and } x_1^+ \leq x_2^+. \quad (4.58)$$

From Eq. (4.50), in order for the region where the effective potential $V_1(x)$ is nonpositive to exist, the condition

$$X \leq Z_1^2, \quad (4.59)$$

should be satisfied. We note that since X is nonpositive in the cases I, II, and III, Eq. (4.59) is satisfied trivially. On the other hand, since X is positive in the cases IV and V, Eq. (4.59) gives the minimum of Z_1^2 .

Cases I, II, and III

In these cases, we consider the region $x_2^H \leq x \leq x_1^+$ as in the case of the particle collision. As x increases from x_2^H to x_1^+ , the CM energy begins with

$$E_{\text{cm}}(x_2^H) = \sqrt{\mu_1^2 + \mu_2^2 + \mu_1\mu_2 \left(\frac{Z_2}{|Z_1|} + \frac{|Z_1|}{Z_2} \right)}, \quad (4.60)$$

and monotonically increases to $E_{\text{cm}}(x_1^+) = E_{\text{cm}}^{\text{max}}$, where

$$E_{\text{cm}}^{\text{max}} \equiv \sqrt{\mu_1^2 + \mu_2^2 + 2\mu_1\mu_2 \frac{Z_2}{|Z_1|}}. \quad (4.61)$$

We have used the l'Hopital's rule to estimate $E_{\text{cm}}(x_2^H)$. In a critical limit $Z_1 \rightarrow 0$, both $E_{\text{cm}}(x_2^H)$ and $E_{\text{cm}}(x_1^+)$ become arbitrarily large and x_1^+ coincides with x_2^H . This behavior of the CM energy and results are similar to those of particle collision in the critical limit $e_i \rightarrow 0$.

The significant difference between the shell collision and the particle collision is that the event horizon x_3^H exists outside the collision point because of the self-gravity of shell 2. Thus, an arbitrarily large CM energy cannot be seen by an observer who stands outside the event horizon x_3^H .

Cases IV and V

In these cases, the event horizon x_2^H does not exist. Thus, we consider the region $x_1^- \leq x \leq x_1^+$. As x increases from x_1^- to x_1^+ , the CM energy begins with $E_{\text{cm}}(x_1^-) = E_{\text{cm}}^{\text{max}}$, monotonically decreases to

$$E_{\text{cm}}(x^m) = \sqrt{\mu_1^2 + \mu_2^2 + 2\mu_1\mu_2 \frac{|Z_1|Z_2 - \sqrt{(Z_1^2 - X)(Z_2^2 - X)}}{X}}, \quad (4.62)$$

and monotonically increases to $E_{\text{cm}}(x_1^+) = E_{\text{cm}}^{\text{max}}$.

From Eqs. (4.59), the critical shell with $Z_1 = 0$ is forbidden, since X is positive. When $Z_1 \rightarrow \sqrt{X}$, i.e., $V_1(x^m) = 0$, shell 1 can be only at $x = x^m = x_1^\pm$. Then, the CM energy there is given by

$$E_{\text{cm}}(x = x^m = x_1^\pm) = \sqrt{\mu_1^2 + \mu_2^2 + \frac{2\mu_1\mu_2 Z_2}{\sqrt{X}}}, \quad (4.63)$$

and it is finite.

4.3.2 Observable CM energy

Here, we assume that the D_3 is the BTZ black hole spacetime, i.e., except the class V, and also we assume that an observer stands outside the event horizon x_3^H . We are interested in an observable collision, i.e., a collision occurs in the region $x_3^H \leq x$. A condition $x_3^H \leq x_1^+$ must be satisfied for the existence of shell 1. From Eqs. (4.44) and (4.51), the condition $x_3^H \leq x_1^+$ is expressed as

$$\mu_2 \mathcal{E}_2 \leq Z_1^2. \quad (4.64)$$

From Eqs. (4.61) and (4.64), the finite upper bound of the observable CM energy is given by

$$E_{\text{cm}}(x = x_3^H = x_1^+) = \sqrt{\mu_1^2 + \mu_2^2 + \frac{\mu_1\mu_2(\mu_2 + 4\mathcal{E}_2)}{2\sqrt{\mu_2\mathcal{E}_2}}}. \quad (4.65)$$

This implies that the self-gravity caused by the collision of two shells suppresses the CM energy.

For an equal mass $\mu \equiv \mu_1 = \mu_2$ case, the upper bound becomes

$$E_{\text{cm}} = \frac{\mu^{3/4}}{\sqrt{2}\mathcal{E}_2^{1/4}} \left(2\sqrt{\mathcal{E}_2} + \sqrt{\mu} \right), \quad (4.66)$$

and it becomes

$$E_{\text{cm}} \simeq \sqrt{2}\mathcal{E}_2^{1/4} \mu^{3/4}, \quad (4.67)$$

for a small mass case, where $\mu \ll \mathcal{E}_2$.

4.3.3 Test shell limit

We consider test shell limit for shells 1 and 2

$$\mu_1 \rightarrow 0 \quad \text{and} \quad M_1 \rightarrow \mathcal{M}_- \equiv M_2 \quad \text{with} \quad \mathcal{E}_1 = (\text{const}) \neq 0, \quad (4.68)$$

and

$$\mu_2 \rightarrow 0 \quad \text{and} \quad M_2 \rightarrow \mathcal{M}_+ \equiv M_3 \quad \text{with} \quad \mathcal{E}_2 = (\text{const}) \neq 0, \quad (4.69)$$

respectively.

Here we show that there are two effects of the self-gravity of thin shells. First, the mass of inner shell affects its critical condition:

$$Z_1 = \frac{\mu_1}{4} - \mathcal{E}_1 = 0. \quad (4.70)$$

In the test shell limit for shell 1, the critical condition becomes $\mathcal{E}_1 \rightarrow 0$ and it corresponds to the critical condition for particles Eq. (4.11). Second, the radial position of the event horizon behaves as $x_a^H \rightarrow x_{a+1}^H$ in the test shell limit for shell a .

We can also see the correspondence to the CM energy of particles and shells. From Eq. (4.61), the CM energy of two thin shells with the equal mass μ at $x = x_1^+$ in the test shell limit for shells 1 and 2 is given by

$$\frac{E_{\text{cm}}^2(x_1^+)}{2\mu^2} = 1 + \frac{Z_2}{|Z_1|} \rightarrow 1 + \frac{\mathcal{E}_2}{\mathcal{E}_1}. \quad (4.71)$$

From Eq. (4.10), the CM energy of two particles with the equal mass m at $x = x_1^+$ is given by

$$\frac{E_{\text{cm}}^2(x_1^+)}{2m^2} = 1 + \frac{e_2}{e_1}. \quad (4.72)$$

Furthermore, from Eq. (4.67), the CM energy behaves as

$$\frac{E_{\text{cm}}}{\mu} \simeq \sqrt{2}\mathcal{E}_2^{1/4}\mu^{-1/4} \gg 1, \quad (4.73)$$

for a small mass case, where $\mu \ll \mathcal{E}_2$. Therefore, when we estimate the observable CM energy, we cannot ignore the self-gravity caused by the colliding objects.

These imply that the self-gravity of the shell influences the critical condition, the radial position of the event horizon, and the CM energy all of them. The test shell limit would help us to understand the effect of the self-gravity of the thin shells on the collisions.

For technical reasons, we discussed the shell collision in the BTZ spacetime instead of the particle collision in the Kerr spacetime. However, the BSW like collision occur not only in 4-dimensional spacetimes but also in the BTZ spacetime and the effect of the negative cosmological constant will be negligible since the collision with a high CM energy occurs near an extremal event horizon, we have shown in Chap. 3.

Chapter 5

Collisional Penrose process

We present an analytic formulation to investigate the energy extraction efficiency in the collisional Penrose process. We focus on a collision with arbitrarily large CM energy, which occurs if either of the colliding particles satisfies a certain critical condition. We show that if this particle is ingoing on the collision, the upper limit of the efficiency is $(2 + \sqrt{3})(2 - \sqrt{2}) \simeq 2.186$, while if it is bounced back before the collision, the upper limit of the efficiency is $(2 + \sqrt{3})^2 \simeq 13.93$. For simplicity, we assume that the motion and collision of particles are confined in the equatorial plane of the extremal Kerr black hole, where $\theta = \pi/2$ and $a = M$.

5.1 Particle motion in the Kerr black hole

5.1.1 Geodesic in the equatorial plane

First of all, we consider a particle motion in the equatorial plane of the extremal Kerr black hole. It reduces to a simple one-dimensional potential problem Eq. (2.21) and the radial momentum is expressed as

$$p^r = \sigma \sqrt{-2V(r)}, \quad (5.1)$$

where $V(r)$ is the effective potential of the particle motion and $\sigma \equiv \text{sgn}(p^r) = \pm 1$. The explicit form of $V(r)$ is given by

$$V(r) = -\frac{Mm^2}{r} + \frac{L^2 - M^2(E^2 - m^2)}{2r^2} - \frac{M(L - ME)^2}{r^3} - \frac{E^2 - m^2}{2}, \quad (5.2)$$

where E , L , and m are the energy, angular momentum, and rest mass of the particle, respectively. The particle motion is restricted to a region where $V(r)$ is nonpositive.

The forward-in-time condition $p^t \geq 0$ near the horizon $r \rightarrow r_+ + 0$ reduces to

$$E - \Omega_H L \geq 0, \quad (5.3)$$

where $r_+ = M$ and $\Omega_H = 1/(2M)$ are the horizon radius and the angular velocity of the horizon, respectively. We define a critical angular momentum L_c as

$$L_c \equiv \frac{E}{\Omega_H}. \quad (5.4)$$

We call a particle a critical particle if it has the critical angular momentum. Accordingly, we call a particle with $L < L_c$ ($L > L_c$) a subcritical (supercritical) particle.

The forward-in-time condition for general position $r_+ \leq r$ is expressed as

$$\frac{1}{2} \left[\left(\frac{r}{M} \right)^3 + \frac{r}{M} + 2 \right] E \geq l, \quad (5.5)$$

where $l \equiv L/M$ and the critical angular momentum $l_c \equiv L_c/M$ becomes

$$l_c = 2E. \quad (5.6)$$

5.1.2 Radial turning points

Next, we are concerned with a particle that comes from or escapes to infinity, which requires the effective potential is nonpositive for large r . This requires $E \geq m$.

massless particles

For a massless particle ($m = 0$), solving $V(r) = 0$ for the impact parameter $b \equiv L/E$, we obtain $b = b_{\pm}(r)$, where

$$b_+(r) \equiv r + M, \quad b_-(r) \equiv - \left(r + M + \frac{4M^2}{r - 2M} \right). \quad (5.7)$$

The numerical plot of $b = b_{\pm}(r)$ is given in Fig. 5.1 (a). This implies that a particle with $b = b_{\pm}(r)$ has a turning point at r .

As r increases from M to infinity, $b_+(r)$ begins with $2M$ and monotonically increases to infinity. As r increases from M to $2M$, $b_-(r)$ begins with $2M$ and monotonically increases to infinity. As r increases from $2M$ to infinity, $b_-(r)$ begins with negative infinity, monotonically increases to a local maximum $-7M$ at $r = 4M$ and monotonically decreases to negative infinity.

Therefore, for $2M < b \leq b_+(r_*)$, the particle can escape to infinity irrespective of the sign of the initial velocity, which is shown by the yellow region in Fig. 5.1 (a), where we denote the radial position of the collision as r_* . On the other hand, for $M < r_* < 4M$ and $-7M < b \leq 2M$, the particle can escape to the infinity only if it moves initially outwardly, which is shown by the blue region in Fig. 5.1 (a).

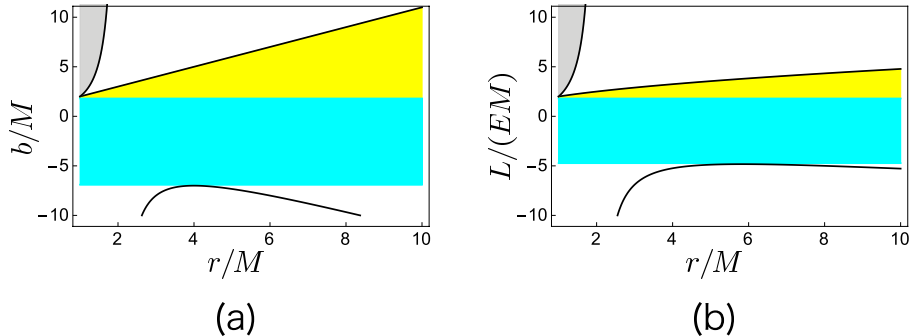


Figure 5.1: The radial turning points are plotted for a massless particle (a) with $b = b_{\pm}(r)$ and for a massive particle (b) with $l = l_{\pm}(r, E, m)$, where we set $E = m = 1$. The negative energy particles are confined to the gray regions.

massive particles

For a massive particle ($m > 0$), solving $V(r) = 0$ for $l = L/M$, we obtain $l = l_{\pm}(r, E, m)$, where

$$l_{\pm}(r, E, m) \equiv \frac{-2M^2E \pm r(r-M)\sqrt{E^2 - m^2 + 2Mm^2/r}}{M(r-2M)}. \quad (5.8)$$

The numerical plot of $l = l_{\pm}(r)$ is given in Fig. 5.1 (b). This implies that a particle with E , m , and $l = l_{\pm}(r, E, m)$ has a turning point at r .

As r increases from M to infinity, $l_+(r, E, m)$ begins with $2E$ and monotonically increases to infinity. As r increases from M to $2M$, $l_-(r, E, m)$ begins with $2E$ and monotonically increases to infinity. As r increases from $2M$ to infinity, $l_-(r, E, m)$ begins with negative infinity, monotonically increases to a local maximum $l_m (< 0)$ at $r = r_m$ and monotonically decreases to negative infinity.

Therefore, for $2E < l \leq l_+(r_*, E, m)$, the particle can escape to infinity irrespective of the sign of the initial velocity, which is shown by the yellow region in Fig. 5.1 (b). On the other hand, for $M < r_* < r_m$ and $l_m < l \leq 2E$, the particle can escape to infinity only if it moves initially outwardly, which is shown by the blue region in Fig. 5.1 (b).

5.2 Particle collision and reaction

Let us consider the reaction of two colliding particles, named particles 1 and 2, to two produced particles, named particles 3 and 4. For each particle i ($i = 1, 2, 3, 4$), we write p^μ , E , l , m and σ as p_i^μ , E_i , l_i , m_i , and σ_i , respectively. We assume that particle 1 and 2 come from infinity, particle 3 escape to infinity, and particle 4 is a negative energy particle, i.e., $E_4 < 0$.

The local conservation of the 4-momenta can be written as

$$p_1^\mu + p_2^\mu = p_3^\mu + p_4^\mu. \quad (5.9)$$

The t - and φ -components of Eq. (5.9) represent the conservations of energy and angular momentum

$$E_1 + E_2 = E_3 + E_4, \text{ and } l_1 + l_2 = l_3 + l_4, \quad (5.10)$$

respectively. The r -component represents the conservation of the radial momentum

$$\sigma_1 |p_1^r| + \sigma_2 |p_2^r| = \sigma_3 |p_3^r| + \sigma_4 |p_4^r|. \quad (5.11)$$

We note that there are four parameters (E, l, m, σ) for each particle. We have three conservation equations and so $4 \times 4 - 3 = 13$ degrees of freedom are remaining. If we specify the parameters of the incident particles, we can fix $(E_1, l_1, m_1, \sigma_1)$ and $(E_2, l_2, m_2, \sigma_2)$. Thus, $13 - 8 = 5$ degrees of freedom are remaining. Moreover, we can fix (m_3, σ_3) and (m_4, σ_4) for a particle reaction we know. Thus, only one degree of freedom is remaining. We express this degree of freedom as parameter δ and use it for an escape particle, where δ parameterizes the ratio of E and l , i.e.,

$$l = E(2 + \delta). \quad (5.12)$$

Clearly, we cannot control δ , which corresponds to the direction of the initial velocities of the product particles.

5.2.1 Particle collision on the horizon

From Eqs. (5.1) and (5.2), we obtain the r -component of 4-momentum on the event horizon as

$$|p_i^r| = 2E_i - l_i, \quad (5.13)$$

where we have used the forward-in-time condition to open the square root.

To investigate the collisional Penrose process with an arbitrarily large CM energy, we assume particle 1 to be critical, i.e., $2E_1 - l_1 = 0$, and particle 2 to be subcritical, i.e., $2E_2 - l_2 > 0$. We also assume that particle 2 moves inwardly, i.e., $\sigma_2 = -1$, because a subcritical particle does not have a turning point near the event horizon¹, see Fig. 5.1.

Then, Eq. (5.11) is expressed as

$$-(2E_2 - l_2) = \begin{cases} \sigma_3(2E_2 - l_2) & (\text{for } \sigma_3 = \sigma_4) \\ \sigma_3 [2(2E_3 - l_3) - (2E_2 - l_2)] & (\text{for } \sigma_3 = -\sigma_4) \end{cases}, \quad (5.14)$$

and several situations are possible depending on the values of σ_3 and σ_4 .

¹We consider an outgoing subcritical particle in Chap. 6.

- If $\sigma_3 = \sigma_4 = 1$, we obtain $2E_2 - l_2 = 0$, which contradicts our assumption.
- If $\sigma_3 = \sigma_4 = -1$, we obtain a trivial equation, which implies that particle 3 can be either critical or subcritical. Nevertheless, we treat only the critical case because a subcritical ingoing particle cannot escape to infinity.
- If $\sigma_3 = -\sigma_4 = 1$, we obtain $2E_3 - l_3 = 0$, i.e., particle 3 is critical.
- If $\sigma_3 = -\sigma_4 = -1$, we obtain $2E_2 - l_2 = 2E_3 - l_3$, which implies that particle 3 is subcritical. It is not interesting since a subcritical ingoing particle cannot escape to infinity again.

From the above considerations, the following assumptions are interesting for energy extraction.

- Particle 1 is critical $2E_1 - l_1 = 0$, come from infinity, and both $\sigma_1 = \pm 1$.
- Particle 2 is subcritical $2E_2 - l_2 > 0$, come from infinity, and moves inwardly $\sigma_2 = -1$.
- Particle 3 is critical on the horizon, escape to infinity, and both $\sigma_3 = \pm 1$.
- Particle 4 is a negative energy particle, falls into the black hole, and moves inwardly $\sigma_4 = -1$.

5.2.2 Near horizon and near critical behaviors

We assume that the particle collision occurs near the event horizon. We introduce the radial position of near-horizon collision r_* as

$$r_* = \frac{M}{1 - \epsilon}, \quad 0 < \epsilon \ll 1. \quad (5.15)$$

We take the energy and angular momentum of the escaping particle as functions of those of the incident particles, the collision point r_* , and δ , i.e.,

$$E_3 = E_3(E_1, l_1, m_1, \sigma_1; E_2, l_2, m_2, \sigma_2; m_3, \sigma_3; m_4, \sigma_4; \delta; r_*), \quad (5.16)$$

$$l_3 = l_3(E_1, l_1, m_1, \sigma_1; E_2, l_2, m_2, \sigma_2; m_3, \sigma_3; m_4, \sigma_4; \delta; r_*). \quad (5.17)$$

Since E_3 and l_3 are function of r_* , we can assume that E_3 and l_3 are expandable in terms of ϵ as

$$E_3 = E_{3(0)} + E_{3(1)}\epsilon + E_{3(2)}\epsilon^2 + O(\epsilon^3), \quad (5.18)$$

$$l_3 = l_{3(0)} + l_{3(1)}\epsilon + l_{3(2)}\epsilon^2 + O(\epsilon^3), \quad (5.19)$$

We expand E_i and l_i in terms of ϵ for the product particles $i = 3, 4$, but not for the incident particles $i = 1, 2$. This looks asymmetric but is suitable for the present physical setting. Equivalently, instead of l_3 , it is more convenient to expand δ as

$$\delta = \delta_{(1)}\epsilon + \delta_{(2)}\epsilon^2 + O(\epsilon^3). \quad (5.20)$$

Therefore, we regard particle 3 as near-critical in the near-horizon collision and the near-critical angular momentum is given by

$$\begin{aligned}
l_3 &= E_3(2 + \delta) \\
&= 2E_{3(0)} + (E_{3(0)}\delta_{(1)} + 2E_{3(1)})\epsilon \\
&\quad + (E_{3(0)}\delta_{(2)} + E_{3(1)}\delta_{(1)} + 2E_{3(2)})\epsilon^2 + O(\epsilon^3).
\end{aligned} \tag{5.21}$$

From Eqs. (5.8), (5.15), and (5.18), we obtain

$$l_+(r_*, E_3, m_3) = 2E_{3(0)} + \left(2E_{3(0)} + 2E_{3(1)} - \sqrt{E_{3(0)}^2 - m_3^2}\right)\epsilon + O(\epsilon^2). \tag{5.22}$$

If particle 3 moves initially inwardly with $E_3 \geq m_3$ and to escape to infinity, it must be bounced back by the effective potential, i.e., $2E_3 < l_3 \leq l_+(r_*, E_3, m_3)$ must be satisfied. This implies

$$0 < \delta_{(1)} \leq \delta_{(1),\max} \equiv \frac{2E_{3(0)} - \sqrt{E_{3(0)}^2 - m_3^2}}{E_{3(0)}}. \tag{5.23}$$

If particle 3 moves initially outwardly with $E_3 \geq m_3$, it always can escape to infinity.

From Eqs. (5.5), (5.15), and (5.18), the forward-in-time condition for particle 3 in the near-horizon implies

$$l_3 < 2E_{3(0)} + 2(E_{3(0)} + E_{3(1)})\epsilon + O(\epsilon^2). \tag{5.24}$$

Therefore, when $l_3 \leq l_+(r_*, E_3, m_3)$, the forward-in-time condition is always satisfied.

5.2.3 Expansion of the radial momentum

We consider the series expansion of the radial momentum in powers of ϵ for each particle. Since we have assumed particle 1 to be critical, particle 2 to be subcritical, and particle 3 to be near-critical, the radial momentum for each

particles are expanded as

$$|p_1^r| = \sqrt{3E_1^2 - m_1^2} \epsilon - \frac{E_1^2}{\sqrt{3E_1^2 - m_1^2}} \epsilon^2 + O(\epsilon^3), \quad (5.25)$$

$$|p_2^r| = (2E_2 - l_2) - 2(E_2 - l_2)\epsilon + \frac{(3E_2 - l_2)(E_2 - l_2) - m_2^2}{2(2E_2 - l_2)} \epsilon^2 + O(\epsilon^3), \quad (5.26)$$

$$\begin{aligned} |p_3^r| &= \sqrt{E_{3(0)}^2 (3 - \delta_{(1)}) (1 - \delta_{(1)}) - m_3^2} \epsilon \\ &+ \frac{E_{3(0)}^2 [-1 + (2 - \delta_{(1)}) (2\delta_{(1)} - \delta_{(2)})] + E_{3(0)} E_{3(1)} (3 - \delta_{(1)}) (1 - \delta_{(1)})}{\sqrt{E_{3(0)}^2 (3 - \delta_{(1)}) (1 - \delta_{(1)}) - m_3^2}} \epsilon^2 \\ &+ O(\epsilon^3), \end{aligned} \quad (5.27)$$

$$\begin{aligned} |p_4^r| &= (2E_2 - l_2) + [2E_1 - 2(E_2 - l_2) - E_{3(0)} (2 - \delta_{(1)})] \epsilon \\ &+ \left[\frac{2E_2 - l_2}{2} - E_{3(0)} (2\delta_{(1)} - \delta_{(2)}) - E_{3(1)} (2 - \delta_{(1)}) \right. \\ &\quad \left. - \frac{(E_1 + E_2 - E_{3(0)})^2 + m_4^2}{2(2E_2 - l_2)} \right] \epsilon^2 + O(\epsilon^3). \end{aligned} \quad (5.28)$$

5.3 Energy extraction efficiency

Let us estimate the maximum value of the energy-extraction efficiency by using the expanded radial momentum and its conservation. Since we have assumed that particle 2 and 4 move inwardly, i.e., $\sigma_2 = \sigma_4 = -1$, the radial momentum conservation is expressed as

$$\sigma_1 |p_1^r| - |p_2^r| = \sigma_3 |p_3^r| - |p_4^r|, \quad (5.29)$$

where $\sigma_1 = -1$ and $\sigma_1 = 1$ correspond to the BSW process [1] and the Schnittman process [49], respectively. Since we have expanded E_3 in terms of ϵ , η is expressed as

$$\eta^{(\sigma_1)(\sigma_3)} = \frac{E_{3(0)}}{E_1 + E_2}, \quad (5.30)$$

where superscripts denote the signs of σ_1 and σ_3 . For example, $\eta^{(+)(-)}$ denote the efficiency when choose $\sigma_1 = 1$ and $\sigma_3 = -1$.

5.3.1 First order of the radial momentum conservation

Since the terms of $O(1)$ in Eq. (5.29) is already considered, we proceed to the terms of $O(\epsilon)$ in the same equation. From Eqs. (5.25)–(5.28), we obtain

$$A - E_{3(0)} (2 - \delta_{(1)}) = \sigma_3 \sqrt{E_{3(0)}^2 (3 - \delta_{(1)}) (1 - \delta_{(1)}) - m_3^2}, \quad (5.31)$$

where $A \equiv 2E_1 + \sigma_1 \sqrt{3E_1^2 - m_1^2} > 0$. Squaring the both sides of Eq. (5.31), we find

$$2 - \delta_{(1)} = \frac{A^2 + E_{3(0)}^2 + m_3^2}{2AE_{3(0)}}. \quad (5.32)$$

Substituting the above expression into Eq. (5.31), we obtain

$$A - \frac{E_{3(0)}^2 + m_3^2}{A} = 2\sigma_3 \sqrt{E_{3(0)}^2 (3 - \delta_{(1)}) (1 - \delta_{(1)}) - m_3^2}. \quad (5.33)$$

This implies $E_{3(0)} \leq \lambda_0 \equiv \sqrt{A^2 - m_3^2}$ ($E \geq \lambda_0$) for $\sigma_3 = 1$ ($\sigma_3 = -1$).

If we choose $\sigma_3 = -1$, $\delta_{(1)} \geq 0$ must be satisfied for particle 3 to escape to infinity. Supposing $\delta_{(1)} \geq 0$ in Eq. (5.32), we have

$$E_{3(0)}^2 - 4AE_{3(0)} + A^2 + m_3^2 \leq 0. \quad (5.34)$$

Thus, we find

$$\lambda_- \leq E_{3(0)} \leq \lambda_+, \quad \lambda_{\pm} \equiv 2A \pm \sqrt{3A^2 - m_3^2}, \quad (5.35)$$

where $E_{3(0)} = \lambda_+$ is realized only for $\delta_{(1)} = 0$.

Therefore, the maximum efficiency is given by

$$\eta^{(\sigma_1)(+)} = \frac{\sqrt{\left(2E_1 + \sigma_1 \sqrt{3E_1^2 - m_1^2}\right)^2 - m_3^2}}{E_1 + E_2}, \quad (5.36)$$

for $\sigma_3 = 1$ while

$$\eta^{(\sigma_1)(-)} = \frac{2 \left(2E_1 + \sigma_1 \sqrt{3E_1^2 - m_1^2}\right) + \sqrt{3 \left(2E_1 + \sigma_1 \sqrt{3E_1^2 - m_1^2}\right)^2 - m_3^2}}{E_1 + E_2}, \quad (5.37)$$

for $\sigma_3 = -1$. We note that λ_+ is always greater than λ_0 , i.e., the upper limit of η for $\sigma_3 = -1$ is always greater than that for $\sigma_3 = 1$.

5.3.2 Second order of the radial momentum conservation

The terms of $O(\epsilon^2)$ in Eq. (5.29) yield

$$\begin{aligned} & \sigma_1 \frac{E_1^2}{\sqrt{3E_1^2 - m_1^2}} + \frac{(3E_2 - l_2)(E_2 - l_2) - m_2^2}{2(2E_2 - l_2)} \\ &= \sigma_3 \frac{E_{3(0)}^2 [-1 + (2 - \delta_{(1)}) (2\delta_{(1)} - \delta_{(2)})] + E_{3(0)} E_{3(1)} (3 - \delta_{(1)}) (1 - \delta_{(1)})}{\sqrt{E_{3(0)}^2 (3 - \delta_{(1)}) (1 - \delta_{(1)}) - m_3^2}} \\ & \quad + \frac{2E_2 - l_2}{2} - E_{3(0)} (2\delta_{(1)} - \delta_{(2)}) - E_{3(1)} (2 - \delta_{(1)}) - \frac{(E_1 + E_2 - E_{3(0)})^2 + m_4^2}{2(2E_2 - l_2)}. \end{aligned} \quad (5.38)$$

From the above equation, if we fix $E_{3(0)}$ and $\delta_{(1)}$, we find the relation between $E_{3(1)}$ and $\delta_{(2)}$. Since both $E_{3(1)}$ and $\delta_{(2)}$ appear only linearly, we can always solve the above equation for $E_{3(1)}$ in terms of $\delta_{(2)}$. Thus, we do not obtain any additional condition to the lower-order terms.

5.3.3 Maximum efficiency

The BSW process: $\sigma_1 = -1$

From Eqs. (5.36) and (5.37), the efficiency for $\sigma_3 = 1$ and $\sigma_3 = -1$ are given by

$$\eta^{(-)(+)} = \frac{\sqrt{\left(2E_1 - \sqrt{3E_1^2 - m_1^2}\right)^2 - m_3^2}}{E_1 + E_2}, \quad (5.39)$$

and

$$\eta^{(-)(-)} = \frac{2\left(2E_1 - \sqrt{3E_1^2 - m_1^2}\right) + \sqrt{3\left(2E_1 - \sqrt{3E_1^2 - m_1^2}\right)^2 - m_3^2}}{E_1 + E_2}, \quad (5.40)$$

respectively. Here we still take m_i as fixed parameters but E_1 and E_2 as free ones in the ranges $E_1 \geq m_1$ and $E_2 \geq m_2$, respectively. The maximum efficiency is attained for $E_1 = m_1$ and $E_2 = m_2$. In this case, we obtain

$$\eta^{(-)(+)} = \frac{\sqrt{(2 - \sqrt{2})^2 m_1^2 - m_3^2}}{m_1 + m_2}, \quad (5.41)$$

which is less than unity, and

$$\eta^{(-)(-)} = \frac{2(2 - \sqrt{2})m_1 + \sqrt{3(2 - \sqrt{2})^2 m_1^2 - m_3^2}}{m_1 + m_2}. \quad (5.42)$$

From the above expressions, we consider several cases as following. For perfectly elastic collision, $\eta^{(-)(-)} = \frac{7-4\sqrt{2}}{2} < 1$. For pair annihilation, $\eta^{(-)(-)} = \frac{(2-\sqrt{2})(2+\sqrt{3})}{2} \simeq 1.093$, which agrees very well with the numerical result in Ref. [47]. For inverse Compton with $m_2 = m_3 = 0$, $\eta^{(-)(-)} = (2 - \sqrt{2})(2 + \sqrt{3}) \simeq 2.186$.

The Schnittman process: $\sigma_1 = 1$

From Eqs. (5.36) and (5.37), the efficiency for $\sigma_3 = 1$ and $\sigma_3 = -1$ are given by

$$\eta^{(+)(+)} = \frac{\sqrt{\left(2E_1 + \sqrt{3E_1^2 - m_1^2}\right)^2 - m_3^2}}{E_1 + E_2}, \quad (5.43)$$

and

$$\eta^{(+)(-)} = \frac{2 \left(2E_1 + \sqrt{3E_1^2 - m_1^2} \right) + \sqrt{3 \left(2E_1 + \sqrt{3E_1^2 - m_1^2} \right)^2 - m_3^2}}{E_1 + E_2}, \quad (5.44)$$

respectively. For the Schnittman process, the situation is very different and much simpler. The maximum efficiency can be attained for $E_1 \gg \max(m_1, m_3)$ and $E_1 \gg E_2$. In this case, we find

$$\eta_{\max}^{(+)(+)} = 2 + \sqrt{3} \simeq 3.732, \quad (5.45)$$

$$\eta_{\max}^{(+)(-)} = \left(2 + \sqrt{3} \right)^2 \simeq 13.93. \quad (5.46)$$

The latter is a universal maximum efficiency irrespective of the details of the particle reaction or the masses of the particles.

Chapter 6

Arbitrarily large energy extraction and escape probability

We present an analytic formulation to investigate the energy extraction efficiency and the escape probability in the super-Penrose process. We consider the situation where two massive particles, named particles 1 and 2, collide head-on in the equatorial plane of the extremal Kerr black hole and produce two massless particles, named particles 3 and 4. Focusing on a typical case, where both of the colliding particles have zero angular momenta, we show that a massless particle produced in such a collision can escape to infinity with arbitrarily large energy in the near-horizon limit of the collision point.

Furthermore, if we assume that the emission of the produced massless particles is isotropic in the center-of-mass frame but confined to the equatorial plane, the escape probability of the produced massless particle approaches $5/12$, and almost all escaping massless particles have arbitrarily large energy at infinity and an impact parameter approaching $2M$, where M is the mass of the black hole.

6.1 Particle collision and escape cone

From Eq. (2.1), the metric in the equatorial plane of the extremal Kerr black hole is given by

$$ds^2 = - \left(1 - \frac{2M}{r}\right) dt^2 - \frac{4M^2}{r} dt d\varphi + \left(\frac{r}{r-M}\right)^2 dr^2 + A(r) d\varphi^2, \quad (6.1)$$

where $A(r) \equiv r^2 + M^2 + 2M^3/r$. The radius of the horizon and ergoregion are given by $r = r_+ \equiv M$ and $r = r_E \equiv 2M$. From Eq. (2.12)–(2.15), the

components of the 4-momentum p^μ are given by

$$p^t = \frac{1}{(r-M)^2} \left[A(r)E - \frac{2M^2}{r}L \right], \quad (6.2)$$

$$p^r = \sigma \sqrt{-2V(r)}, \quad (6.3)$$

$$p^\theta = 0, \quad (6.4)$$

$$p^\varphi = \frac{1}{(r-M)^2} \left[\frac{2M^2}{r}E + \left(1 - \frac{2M}{r} \right) L \right], \quad (6.5)$$

where E , L , m , and $V(r)$ are the energy, angular momentum, rest mass, and effective potential of the particle, respectively, and $\sigma \equiv \text{sgn}(p^r) = \pm 1$. Here the explicit form of $V(r)$ is given by

$$V(r) = -\frac{Mm^2}{r} + \frac{L^2 - M^2(E^2 - m^2)}{2r^2} - \frac{M(L - ME)^2}{r^3} - \frac{E^2 - m^2}{2}. \quad (6.6)$$

A locally nonrotating frame (LNRF) is a tetrad basis associated with observers who have zero angular momentum. The transformation that relates the components of an arbitrarily vector v^μ to the components in the LNRF $v^{(\alpha)}$ is given by

$$v^{(\alpha)} = e_\mu^{(\alpha)} v^\mu, \quad (6.7)$$

where $e_\mu^{(\alpha)}$ is the tetrad basis of the LNRF. According to Refs. [55, 61], the components of $e_\mu^{(\alpha)}$ are given by

$$e_\mu^{(t)} = \left(\frac{r-M}{\sqrt{A(r)}}, 0, 0, 0 \right), \quad (6.8)$$

$$e_\mu^{(r)} = \left(0, \frac{r}{r-M}, 0, 0 \right), \quad (6.9)$$

$$e_\mu^{(\theta)} = (0, 0, r, 0), \quad (6.10)$$

$$e_\mu^{(\varphi)} = \left(-\frac{2M^2}{r\sqrt{A(r)}}, 0, 0, \sqrt{A(r)} \right). \quad (6.11)$$

These satisfy $g_{\mu\nu} = \eta_{(\alpha)(\beta)} e_\mu^{(\alpha)} e_\nu^{(\beta)}$, where $\eta_{(\alpha)(\beta)} = \text{diag}(-1, 1, 1, 1)$. From Eqs. (6.2)–(6.11), the components of the 4-momentum in the LNRF are given by

$$p^{(\mu)} = \left(\frac{A(r)E - 2M^2L/r}{(r-M)\sqrt{A(r)}}, \sigma \frac{r\sqrt{-2V(r)}}{r-M}, 0, \frac{L}{\sqrt{A(r)}} \right). \quad (6.12)$$

We consider the situation where two massive particles, named particles 1 and 2, collide head-on in the equatorial plane of the extremal Kerr black hole and produce two massless particles, named particles 3 and 4. For each particle i ($i = 1, 2, 3, 4$), we write $p^{(\mu)}$, E , L , m , $V(r)$, and σ as $p_i^{(\mu)}$, E_i , L_i , m_i , $V_i(r)$,

and σ_i , respectively. The components of the total 4-momentum of two colliding particles in the LNRF are obtained as

$$p_1^{(\mu)} + p_2^{(\mu)} = (T, R, 0, \Phi), \quad (6.13)$$

where

$$T \equiv p_1^{(t)} + p_2^{(t)} = \frac{A(r)(E_1 + E_2) - 2M^2(L_1 + L_2)/r}{(r - M)\sqrt{A(r)}}, \quad (6.14)$$

$$R \equiv p_1^{(r)} + p_2^{(r)} = \frac{r}{r - M} \left(\sigma_1 \sqrt{-2V_1(r)} + \sigma_2 \sqrt{-2V_2(r)} \right), \quad (6.15)$$

$$\Phi \equiv p_1^{(\varphi)} + p_2^{(\varphi)} = \frac{L_1 + L_2}{\sqrt{A(r)}}. \quad (6.16)$$

We note that T is always positive because of the forward-in-time condition.

Without loss of generality, we assume that particle 1 moves radially outward, while particle 2 moves radially inward. For simplicity, we assume that particles 1 and 2 have the same mass and zero angular momenta and are marginally bound

$$\sigma_1 = -\sigma_2 = 1, \quad (6.17)$$

$$L_1 = L_2 = 0, \quad (6.18)$$

$$E_1 = m_1 = E_2 = m_2 \equiv m. \quad (6.19)$$

In this case, the spatial components of the total 4-momentum $p_1^{(I)} + p_2^{(I)}$ ($I = r, \theta, \varphi$) vanish. Thus, the LNRF coincides with the center-of-mass frame (CMF) and $p_1^{(t)} + p_2^{(t)}$ yields the CM energy. When we denote the radial position of the collision as r_* , where $M < r_* \leq 2M$, i.e., we assume that the collision occurs in the ergoregion, the CM energy is expressed as

$$E_{\text{cm}} \equiv \sqrt{-\eta_{(\mu)(\nu)} \left(p_1^{(\mu)} + p_2^{(\mu)} \right) \left(p_1^{(\nu)} + p_2^{(\nu)} \right)} = \frac{2m\sqrt{A(r_*)}}{r_* - M}. \quad (6.20)$$

The local conservation of the 4-momenta can be written as

$$p_1^{(\mu)} + p_2^{(\mu)} = p_3^{(\mu)} + p_4^{(\mu)} = E_{\text{cm}}(1, 0, 0, 0). \quad (6.21)$$

From the above equations, the 4-momenta of the two massless particles 3 and 4 moving on the equatorial plane can be written as

$$p_3^{(\mu)} = \frac{E_{\text{cm}}}{2} (1, \cos \alpha, 0, \sin \alpha), \quad (6.22)$$

$$p_4^{(\mu)} = \frac{E_{\text{cm}}}{2} (1, -\cos \alpha, 0, -\sin \alpha). \quad (6.23)$$

This implies that the spatial velocity of particle 3 makes an angle α with $e_\mu^{(r)}$,

where $-\pi \leq \alpha < \pi$. From the components of the 4-momentum, we obtain

$$\sin \alpha = \frac{p_3^{(\varphi)}}{\sqrt{\left(p_3^{(r)}\right)^2 + \left(p_3^{(\varphi)}\right)^2}} = \frac{b(r_* - M)}{A(r_*) - 2M^2b/r_*}, \quad (6.24)$$

$$\cos \alpha = \frac{p_3^{(r)}}{\sqrt{\left(p_3^{(r)}\right)^2 + \left(p_3^{(\varphi)}\right)^2}} = \frac{\sigma_3 r_* \sqrt{A(r_*)}}{A(r_*) - 2M^2b/r_*} \sqrt{1 - \frac{b^2 - M^2}{r_*^2} + \frac{2M(b - M)^2}{r_*^3}}, \quad (6.25)$$

where we have defined $b \equiv L_3/E_3$.

Now we consider the escape of particle 3 from near the horizon to infinity. We define an escape cone S , which is the range of angles in the CMF along which particle 3 must be emitted to escape to infinity. The condition for particle 3 to escape to infinity is determined by investigating a radial turning point, i.e., $V_3(r) = 0$. Solving $V_3(r) = 0$ for b , we obtain $b = b_{\pm}(r)$, where

$$b_+(r) \equiv r + M, \quad b_-(r) \equiv -\left(r + M + \frac{4M^2}{r - 2M}\right). \quad (6.26)$$

This means that particle 3 with impact parameter $b = b_{\pm}(r)$ has the turning point at r , see Sec 5.1.2 for more detail. The numerical plot of $b = b_{\pm}(r)$ is given in Fig. 6.1. For $2M < b \leq b_+(r_*)$, particle 3 can escape to infinity irrespective of the sign of σ_3 . On the other hand, for $-7M < b \leq 2M$, particle 3 can escape to infinity only if $\sigma_3 = 1$ is chosen.

We define critical angles as the boundaries of the impact parameters to escape to infinity:

$$\alpha_{\text{I}} \equiv \alpha(\sigma_3 = -1, r = r_*, b = 2M), \quad (6.27)$$

$$\alpha_{\text{II}} \equiv \alpha(\sigma_3 = -1, r = r_*, b = b_+(r_*)), \quad (6.28)$$

$$\alpha_{\text{III}} \equiv \alpha(\sigma_3 = 1, r = r_*, b = b_+(r_*)), \quad (6.29)$$

$$\alpha_{\text{IV}} \equiv \alpha(\sigma_3 = 1, r = r_*, b = -7M). \quad (6.30)$$

From Eqs. (6.24)–(6.30), we find

$$\sin \alpha_{\text{I}} > 0, \quad \cos \alpha_{\text{I}} < 0, \quad (6.31)$$

$$\sin \alpha_{\text{II}} = \sin \alpha_{\text{III}} = 1, \quad (6.32)$$

$$\sin \alpha_{\text{IV}} < 0, \quad \cos \alpha_{\text{IV}} > 0. \quad (6.33)$$

Therefore, we can find

$$\alpha_{\text{IV}} < \alpha_{\text{III}} = \alpha_{\text{II}} < \alpha_{\text{I}}. \quad (6.34)$$

This means that the escape cone S is given by

$$\alpha \in (\alpha_{\text{IV}}, \alpha_{\text{I}}). \quad (6.35)$$

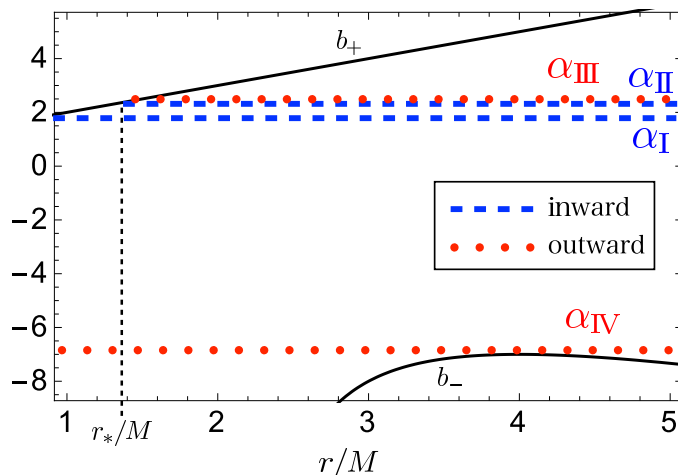


Figure 6.1: The condition for particle 3 to escape to infinity is determined by investigating a radial turning point, i.e., $V_3 = 0$. Solving $V_3 = 0$ for the impact parameter b , we obtain $b = b_{\pm}(r)$. The radial turning points for particle 3 with $b = b_{\pm}(r)$ are plotted by the black solid lines. The range of b where particle 3 can escape from $r = r_*$ to infinity depends on whether it moves initially radially inward or outward. If particle 3 moves initially inward, the maximum and minimum values of b with which particle 3 can escape to infinity are given by the blue dashed lines labeled α_{II} and α_{I} . The values of the blue dashed lines labeled α_{II} and α_{I} are given by $b_+(r_*)/M$ and 2, respectively. If particle 3 moves initially outward, the maximum and minimum values of b with which particle 3 can escape to infinity are given by the red dotted lines labeled α_{III} and α_{IV} . The values of the red dotted lines labeled α_{III} and α_{IV} are given by $b_+(r_*)/M$ and -7 , respectively. Please notice that the blue dashed line labeled α_{II} and the red dotted line labeled α_{III} take the same value, i.e., $\alpha_{\text{II}} = \alpha_{\text{III}}$.

The escape probability P is given by the ratio of the angle of the escape cone to 2π if we assume that particle 3 is emitted isotropically in the CMF and confined to the equatorial plane. It is given by

$$P \equiv \frac{S}{2\pi} = \frac{\alpha_{\text{I}} - \alpha_{\text{IV}}}{2\pi}. \quad (6.36)$$

6.2 Super-Penrose process and escape probability

The components of the time-translational Killing vector ξ^μ in the Boyer-Lindquist coordinates are given by $\xi^\mu = (1, 0, 0, 0)$. Using Eq. (6.7), its components in

the CMF are given by

$$\xi^{(\mu)} = \left(\frac{r-M}{\sqrt{A(r)}}, 0, 0 - \frac{2M^2/r}{\sqrt{A(r)}} \right). \quad (6.37)$$

From Eqs. (6.20), (6.22), (6.24), (6.25), and (6.37), E_3 is given by

$$E_3 \equiv -\eta_{(\mu)(\nu)} \xi^{(\mu)} p_3^{(\nu)} = m \left(1 + \frac{2M^2}{r_*(r_* - M)} \sin \alpha \right). \quad (6.38)$$

Therefore, the energy extraction efficiency is given by

$$\eta \equiv \frac{E_3}{E_1 + E_2} = \frac{1}{2} \left(1 + \frac{2M^2}{r_*(r_* - M)} \sin \alpha \right). \quad (6.39)$$

Because the Killing vector ξ^μ becomes spacelike inside the ergoregion, the conserved energy E_4 can be negative. Thus, if α satisfies

$$\sin \alpha > \frac{r_*(r_* - M)}{2M^2}, \quad (6.40)$$

the energy extraction efficiency can be larger than unity, i.e., the collisional Penrose process occur.

We assume that the collision point is near the horizon and its radial position is given by

$$r_* = \frac{M}{1 - \epsilon}, \quad 0 < \epsilon \ll 1. \quad (6.41)$$

The explicit form of the critical angles is given by

$$\alpha_{\text{I}} = \frac{5\pi}{6} + O(\epsilon), \quad (6.42)$$

$$\alpha_{\text{II}} = \alpha_{\text{III}} = \frac{\pi}{2}, \quad (6.43)$$

$$\alpha_{\text{IV}} = -\frac{7}{18}\epsilon + O(\epsilon^2). \quad (6.44)$$

See Fig. 6.2 for the schematic diagram of the situation.

From Eqs. (6.36), (6.42), and (6.44), the escape probability is obtained as

$$P \rightarrow \frac{5}{12}, \quad (6.45)$$

in the horizon limit $\epsilon \rightarrow 0$. From Eqs. (6.39) and (6.41), if $\sin \alpha = O(1)$, η is given by

$$\eta = \frac{E_3}{2m} = \frac{\sin \alpha}{\epsilon} + O(1), \quad (6.46)$$

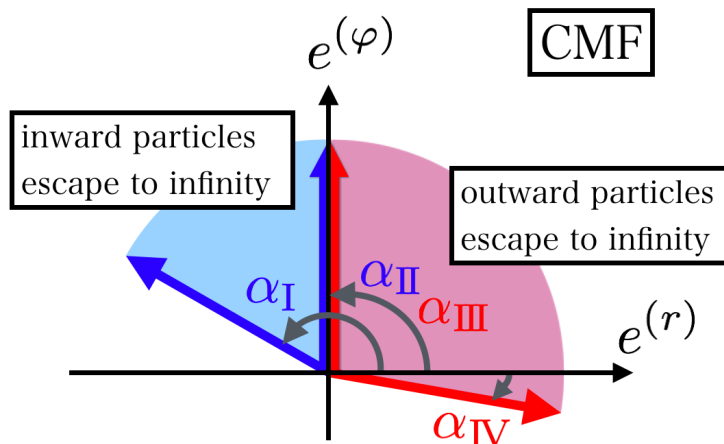


Figure 6.2: The schematic diagram of the critical angles and the escape cone for particle 3, i.e., the range of angles in the CMF along which particle 3 must be emitted to escape from $r = r_*$ to infinity. The colored arrows denote the spatial velocities of particle 3 with the critical angles. The colored sectors denote the escape cone for particle 3. The escape probability is given by the ratio of the angle of the escape cone to 2π . If particle 3 moves initially inward, the maximum and minimum values of α with which particle 3 can escape to infinity are given by α_{I} and α_{II} . Particle 3 emitted radially inward in the range $\alpha \in (\alpha_{\text{II}}, \alpha_{\text{I}})$ bounces back at the turning point and can escape to infinity. If particle 3 moves initially outward, the maximum and minimum values of α with which particle 3 can escape to infinity are given by α_{III} and α_{IV} . Particle 3 emitted radially outward in the range $\alpha \in (\alpha_{\text{IV}}, \alpha_{\text{III}})$ can directly escape to infinity. Since $\alpha_{\text{II}} = \alpha_{\text{III}}$, we represent the spatial velocities of particle 3 with α_{II} and α_{III} as the one arrow colored half blue and half red.

and this diverges to infinity in the limit $\epsilon \rightarrow 0$. Only if $\sin \alpha = O(\epsilon)$, η turns out to be finite. If particle 3 is emitted along the angle α_{IV} , η becomes

$$\eta = \frac{E_3}{2m} = \frac{1}{9} + O(\epsilon). \quad (6.47)$$

This means that the proportion of the particles with finite energy is minuscule. In other words, almost all the particles which escape to infinity have arbitrarily large energy.

From Eqs. (6.24) and (6.41), the relation among the emission angle α , impact parameter b , and ϵ is given by

$$2M - b = \frac{b}{2 \sin \alpha} \epsilon + O(\epsilon^2), \quad (6.48)$$

if $\sin \alpha = O(1)$. Therefore, almost all the particles which escape to infinity have an impact parameter $b = 2M + O(\epsilon)$.

Here, we focus on a special set of parameter values of the colliding particles where particles 1 and 2 have the same mass and zero angular momenta and are marginally bound. However, we would like to stress that it is not a singular example but a typical one which provides a picture that we believe is representative of more general collisions in the super-Penrose process. Even if we do not assume the above assumptions, the escape probability takes a value of the order of unity and almost all the escaping particles have arbitrarily large energy except for the sets of fine-tuned parameter values.

Chapter 7

Conclusions

In this thesis, we have studied a collision of two geodesic particles and dust thin shells in the Bañados-Teitelboim-Zanelli (BTZ) spacetime and an energy extraction by using a particle collision in the Kerr black hole spacetime.

In Chap. 3, we have investigated the collision of two particles in the BTZ black hole spacetime with the negative cosmological constant and angular momentum. We have obtained a general formula for the CM energy of two geodesic particles in the BTZ black hole spacetime. We have shown that the CM energy of two ingoing particles in the near horizon limit can be arbitrarily large if either of the two particles has a critical angular momentum (3.17) and the other has a noncritical angular momentum. We have shown that the motion of a particle with a subcritical angular momentum is allowed near an extremal BTZ black hole and the CM energy for a rear-end collision at a point near the extremal BTZ black hole can be arbitrarily large in the critical angular momentum limit.

Since colliding particles near horizon have large energy, the self-gravity of the particles affects on the collision. The self-gravity caused by the high energy collision will affect the large CM energy and it will be limited to a finite value. This consideration is shown in Chap. 4 by using a collision of two shells.

In Chap. 4, we have investigated the rear-end collision of two dust thin shells in the rotating BTZ spacetime to investigate the effects of the self-gravity of colliding objects on the high energy collision. The shells divide the BTZ spacetime into three domains and the domains are matched by Darmois-Israel's method. From the junction condition, all the domains must have the same angular momenta J and this implies that the shells and domains corotate.

We have revealed that there are two effects of the self-gravity of thin shells. First, we have shown that the mass of inner shell affects its critical condition (4.54). Second, the position of the event horizon changed from x_1^H to x_3^H because of the masses of two shells.

We have considered the shell collision in five cases according to the value of

J . The cases I ($J < \ell M_1$), II ($J = \ell M_1$), and III ($J = \ell M_2$) would be especially interesting cases because of following reasons. The case I is a usual astrophysical situation as a black hole sub-extremely rotates and two objects collide near its event horizon. In case II, the black hole extremely rotates initially and the collision of two falling shells corresponds with the BSW collision of two particles with an arbitrary high CM energy in the extremal black hole spacetime. In case III, inner shell 1 can be satisfied the critical condition that the effective potential for shell 1 becomes $V_1(x_2^H) = V_1'(x_2^H) = 0$ on the extremal event horizon $x = x_2^H$ as with the BSW process in extremal black hole spacetimes [1, 3]. In cases I-III, the CM energy of the shells can be arbitrarily large if inner shell 1 satisfies the critical condition and if outer shell 2 does not. However, an observer outside the event horizon x_3^H cannot see the products of the collision with the arbitrary large CM energy because it occurs inside the event horizon x_3^H .

An observer at $x \geq x_3^H$ may see products after the collision if a shell collision occurs in a region $x_3^H \leq x$. We have obtained the finite upper bound of the CM energy of the collision in the region $x_3^H \leq x$ (4.65)–(4.67). We have concluded that the self-gravity of colliding objects suppresses its CM energy and the observer in the region $x_3^H \leq x$ can only see the suppressed collision.

We have also found a test shell limit. We have shown that the CM energy and the effective potentials for shells in the test shell limit are very similar to the ones of particles. The test shell limit would help us to understand the effect of the self-gravity of the thin shells on the collisions.

In Chap. 5, we have investigated the particle collision and the energy extraction efficiency, where a critical particle (particle 1) and subcritical particle (particle 2) collide near the event horizon of the extremal Kerr black hole and then two particles are produced, one of which escapes to infinity (particle 3) and another falls into the black hole (particle 4). We have proposed an analytic approach to the collisional Penrose process with the expansion in powers of small parameter ϵ , which is parameterized the near-horizon collision (5.15).

We have considered the series expansion of the radial momentum in powers of ϵ for each particle. By using the expanded radial momentum and its conservation, we have estimated the energy extraction efficiency. We have found that the upper limits of the collisional Penrose process restricted in the equatorial plane of the extremal Kerr black hole are given by $(2 + \sqrt{3})(2 - \sqrt{2}) \simeq 2.186$ and $(2 + \sqrt{3})^2 \simeq 13.93$ for the BSW and Schnittman collision, respectively. The former is realized for inverse Compton scattering, while the latter can be universally attained for the various reaction of particles.

Chap. 6, we have investigated the analytic formulation of the energy extraction efficiency and the escape probability in the super-Penrose process. We have considered the situation where two massive particles, named particles 1 and 2, collide head-on in the equatorial plane of the extremal Kerr black hole and produce two massless particles, named particles 3 and 4.

We have focused a special set of parameter values of the colliding particles, where particles 1 and 2 have the same mass and zero angular momenta and are

marginally bound. In this case, the spatial components of the total 4-momentum of the colliding particles vanish in the LNRF, and hence the LNRF coincides with the CMF. We computed the escape cone, i.e., the range of angles in the CMF along which particles must be emitted to escape to infinity, and computed the escape probability. We showed that the escape probability approaches $5/12$ and almost all the escaping particles have arbitrarily large energy with an impact parameter $b \rightarrow 2M$ in the near-horizon limit of the collision point. We would suggest that very high-energy particles with impact parameter $b \simeq 2M$ are produced by the super-Penrose process and can be in principle observed from rapidly rotating black holes in astrophysics.

In this thesis, we have compared the shell collision and the particle collision in the BTZ spacetime in order to investigate the effects of the self-gravity of colliding objects on the high CM energy collision. Since we have shown the self-gravity of colliding objects suppresses its CM energy, next we need to verify the effect on the energy extraction efficiency. The energy extraction by using the collision of two spherical charged shells in the Reissner-Nordström black hole spacetime is founded by Nakao *et al.* [65]. Thus, we need to investigate the energy extraction by using the shell collision in the rotating black hole spacetime.

Acknowledgements

I would like to express the deepest appreciation to professor Tomohiro Harada for insightful suggestions, comments, discussions, and collaborations. I have learned many things from him as a researcher. I am grateful to my collaborators U. Miyamoto, T. Igata, N. Tsukamoto, N. Tanahashi, and Y. Gong for valuable suggestions, comments and discussions. I am also grateful to the examiners T. Kobayashi and K. Ieki for useful suggestions and comments. I would like to thank all the colleagues in Department of Physics in Rikkyo University, especially K. Inagawa, T. Kokubu, S. Yokoyama, T. Hiramatsu, and T. Hirayama. Many thanks to my friends, especially K. Yamada, R. Kase, and Y. Tanaka, for conversations, discussions, and drinking. I sincerely thank my family, Miki, Yuta, Zenya, and Kiyoko. K.O. was supported by JSPS.

Bibliography

- [1] M. Bañados, J. Silk, and S. M. West, “Kerr Black Holes as Particle Accelerators to Arbitrarily High Energy,” *Phys. Rev. Lett.* **103**, 111102 (2009).
- [2] T. Piran, J. Shaham, and J. Katz, “High efficiency of the Penrose mechanism for particle collisions,” *Astrophys. J.* **196**, 107 (1975).
- [3] T. Harada and M. Kimura, “Black holes as particle accelerators: a brief review,” *Class. Quant. Grav.* **31**, 243001 (2014).
- [4] J. D. Schnittman, “The collisional Penrose process,” *Gen. Relativ. Gravit.* **50**, 77 (2018).
- [5] B. P. Abbott *et al.* [LIGO Scientific and Virgo Collaborations], “Observation of Gravitational Waves from a Binary Black Hole Merger,” *Phys. Rev. Lett.* **116**, 061102 (2016).
- [6] E. Berti, V. Cardoso, L. Gualtieri, F. Pretorius, and U. Sperhake, “Comment on ‘Kerr Black Holes as Particle Accelerators to Arbitrarily High Energy’,” *Phys. Rev. Lett.* **103**, 239001 (2009).
- [7] T. Jacobson and T. P. Sotiriou, “Spinning Black Holes as Particle Accelerators,” *Phys. Rev. Lett.* **104**, 021101 (2010).
- [8] S. T. McWilliams, “Black Holes are neither Particle Accelerators nor Dark Matter Probes,” *Phys. Rev. Lett.* **110**, 011102 (2013).
- [9] Kip S. Thorne, Disk accretion on to a black hole. II. Evolution of the hole, *Astrophys. J.* **191**, 507 (1974)
- [10] T. Harada and M. Kimura, “Collision of an innermost stable circular orbit particle around a Kerr black hole,” *Phys. Rev. D* **83**, 024002 (2011).
- [11] T. Harada and M. Kimura, “Collision of an object in the transition from adiabatic inspiral to plunge around a Kerr black hole,” *Phys. Rev. D* **84**, 124032 (2011).
- [12] M. Patil, P. S. Joshi, K. i. Nakao, M. Kimura, and T. Harada, “Timescale for trans-Planckian collisions in Kerr spacetime,” *EPL* **110**, 30004 (2015).

- [13] T. Harada and M. Kimura, “Collision of two general geodesic particles around a Kerr black hole,” *Phys. Rev. D* **83**, 084041 (2011).
- [14] T. Igata, T. Harada, and M. Kimura, “Effect of a Weak Electromagnetic Field on Particle Acceleration by a Rotating Black Hole,” *Phys. Rev. D* **85**, 104028 (2012).
- [15] A. Galajinsky, “Near horizon geometry of extremal black holes and Bañados-Silk-West effect,” *Phys. Rev. D* **88**, 027505 (2013).
- [16] M. Patil and P. S. Joshi, “Kerr Naked Singularities as Particle Accelerators,” *Class. Quant. Grav.* **28**, 235012 (2011).
- [17] S. W. Wei, Y. X. Liu, H. Guo, and C. E. Fu, “Charged spinning black holes as Particle Accelerators,” *Phys. Rev. D* **82**, 103005 (2010).
- [18] Y. Li, J. Yang, Y. L. Li, S. W. Wei, and Y. X. Liu, “Particle Acceleration in Kerr-(anti-) de Sitter Black Hole Backgrounds,” *Class. Quant. Grav.* **28**, 225006 (2011).
- [19] K. Lake, “Particle Accelerators inside Spinning Black Holes,” *Phys. Rev. Lett.* **104**, 211102 (2010), Erratum: [*Phys. Rev. Lett.* **104**, 259903 (2010)].
- [20] J. Yang, Y. L. Li, Y. Li, S. W. Wei, and Y. X. Liu, “Particle collisions in the lower dimensional rotating black hole space-time with the cosmological constant,” *Adv. High Energy Phys.* **2014**, 204016 (2014).
- [21] I. Hussain, “Black holes and collision energy in the center-of-mass frame,” *Mod. Phys. Lett. A* **27**, 1250068 (2012).
- [22] J. Sadeghi, B. Pourhassan, and H. Farahani, “Rotating charged hairy black hole in (2+1) dimensions and particle acceleration,” *Commun. Theor. Phys.* **62**, 358 (2014).
- [23] S. Fernando, “Spinning dilaton black hole in 2+1 dimensions as a particle accelerator,” *Mod. Phys. Lett. A* **32**, 1750074 (2017).
- [24] N. Tsukamoto, K. Ogasawara, and Y. Gong, “Particle collision with an arbitrarily high center-of-mass energy near a Bañados-Teitelboim-Zanelli black hole,” *Phys. Rev. D* **96**, 024042 (2017).
- [25] A. Abdujabbarov, N. Dadhich, B. Ahmedov, and H. Eshkuvatov, “Particle acceleration around a five-dimensional Kerr black hole,” *Phys. Rev. D* **88**, 084036 (2013).
- [26] O. B. Zaslavskii, “Ultrahigh energy particle collisions near many-dimensional black holes: general approach,” *Phys. Rev. D* **90**, 107503 (2014).

- [27] O. B. Zaslavskii, “Acceleration of particles by nonrotating charged black holes,” *JETP Lett.* **92**, 571 (2010) [*Pisma Zh. Eksp. Teor. Fiz.* **92**, 635 (2010)].
- [28] N. Tsukamoto, M. Kimura, and T. Harada, “High energy collision of particles in the vicinity of extremal black holes in higher dimensions: Bañados-Silk-West process as linear instability of extremal black holes,” *Phys. Rev. D* **89**, 024020 (2014).
- [29] M. Kimura, K. i. Nakao, and H. Tagoshi, “Acceleration of colliding shells around a black hole: Validity of the test particle approximation in the Banados-Silk-West process,” *Phys. Rev. D* **83**, 044013 (2011).
- [30] M. Patil, P. S. Joshi, M. Kimura, and K. i. Nakao “Acceleration of particles and shells by Reissner-Nordström naked singularities” *Phys. Rev. D* **86**, 084023 (2012).
- [31] K. i. Nakao, M. Kimura, M. Patil, and P. S. Joshi, “Ultrahigh energy collision with neither black hole nor naked singularity,” *Phys. Rev. D* **87**, 104033 (2013).
- [32] V. De La Cruz and W. Israel, “Spinning Shell as a Source of the Kerr Metric,” *Phys. Rev.* **170**, 1187 (1968).
- [33] J. P. Krisch and E. N. Glass, “Counter-rotating Kerr manifolds separated by a fluid shell,” *Class. Quant. Grav.* **26**, 175010 (2009)
- [34] R. B. Mann, J. J. Oh, and M. I. Park, “The Role of Angular Momentum and Cosmic Censorship in the (2+1)-Dimensional Rotating Shell Collapse,” *Phys. Rev. D* **79**, 064005 (2009).
- [35] T. Delsate, J. V. Rocha, and R. Santarelli, “Collapsing thin shells with rotation,” *Phys. Rev. D* **89**, 121501 (2014).
- [36] J. V. Rocha, “Gravitational collapse with rotating thin shells and cosmic censorship,” *Int. J. Mod. Phys. D* **24**, 1542002 (2015).
- [37] M. Banados, C. Teitelboim, and J. Zanelli, “The Black hole in three-dimensional space-time,” *Phys. Rev. Lett.* **69**, 1849 (1992).
- [38] M. Banados, M. Henneaux, C. Teitelboim, and J. Zanelli, “Geometry of the (2+1) black hole,” *Phys. Rev. D* **48**, 1506 (1993), Erratum: [*Phys. Rev. D* **88**, 069902 (2013)].
- [39] D. Ida, “No black hole theorem in three-dimensional gravity,” *Phys. Rev. Lett.* **85**, 3758 (2000).
- [40] N. Cruz, C. Martinez, and L. Pena, “Geodesic structure of the (2+1) black hole,” *Class. Quant. Grav.* **11**, 2731 (1994).

- [41] J. V. Rocha and V. Cardoso, “Gravitational perturbation of the BTZ black hole induced by test particles and weak cosmic censorship in AdS spacetime,” *Phys. Rev. D* **83**, 104037 (2011).
- [42] J. P. S. Lemos, F. J. Lopes, M. Minamitsuji, and J. V. Rocha, “Thermodynamics of rotating thin shells in the BTZ spacetime,” *Phys. Rev. D* **92**, 064012 (2015).
- [43] J. P. S. Lemos, M. Minamitsuji, and O. B. Zaslavskii, “Thermodynamics of extremal rotating thin shells in an extremal BTZ spacetime and the extremal black hole entropy,” *Phys. Rev. D* **95**, 044003 (2017).
- [44] J. P. S. Lemos, M. Minamitsuji, and O. B. Zaslavskii, “Unified approach to the entropy of an extremal rotating BTZ black hole: Thin shells and horizon limits,” *Phys. Rev. D* **96**, 084068 (2017).
- [45] R. Penrose, “Gravitational collapse: The role of general relativity,” *Riv. Nuovo Cim.* **1**, 252 (1969)
- [46] T. Piran and J. Shaham, “Upper Bounds on Collisional Penrose Processes Near Rotating Black Hole Horizons,” *Phys. Rev. D* **16**, 1615 (1977).
- [47] M. Bejger, T. Piran, M. Abramowicz, and F. Hakanson, “Collisional Penrose process near the horizon of extreme Kerr black holes,” *Phys. Rev. Lett.* **109**, 121101 (2012).
- [48] T. Harada, H. Nemoto, and U. Miyamoto, “Upper limits of particle emission from high-energy collision and reaction near a maximally rotating Kerr black hole,” *Phys. Rev. D* **86**, 024027 (2012), Erratum: [*Phys. Rev. D* **86**, 069902 (2012)].
- [49] J. D. Schnittman, “Revised upper limit to energy extraction from a Kerr black hole,” *Phys. Rev. Lett.* **113**, 261102 (2014).
- [50] E. Leiderschneider and T. Piran, “Maximal efficiency of the collisional Penrose process,” *Phys. Rev. D* **93**, 043015 (2016).
- [51] K. Ogasawara, T. Harada, and U. Miyamoto, “High efficiency of collisional Penrose process requires heavy particle production,” *Phys. Rev. D* **93**, 044054 (2016).
- [52] T. Harada, K. Ogasawara, and U. Miyamoto, “Consistent analytic approach to the efficiency of collisional Penrose process,” *Phys. Rev. D* **94**, 024038 (2016).
- [53] E. Berti, R. Brito, and V. Cardoso, “Ultrahigh-energy debris from the collisional Penrose process,” *Phys. Rev. Lett.* **114**, 251103 (2015).
- [54] K. Ogasawara, T. Harada, U. Miyamoto, and T. Igata, “Escape probability of the super-Penrose process,” *Phys. Rev. D* **95**, 124019 (2017).

- [55] M. Patil, T. Harada, K. Nakao, P. Joshi, and M. Kimura, “Infinite efficiency of the collisional Penrose process: Can a overspinning Kerr geometry be the source of ultrahigh-energy cosmic rays and neutrinos?,” *Phys. Rev. D* **93**, 104015 (2016).
- [56] K. Ogasawara and N. Tsukamoto, “Effect of the self-gravity of shells on a high energy collision in a rotating Bañados-Teitelboim-Zanelli spacetime,” *Phys. Rev. D* **99**, 024016 (2019).
- [57] R. P. Kerr, “Gravitational Field of a Spinning Mass as an Example of Algebraically Special Metrics,” *Phys. Rev. Lett.* **11**, 237 (1963).
- [58] B. Carter, “Global structure of the Kerr family of gravitational fields,” *Phys. Rev.* **174**, 1559 (1968).
- [59] R. M. Wald, *General Relativity*, (University of Chicago Press, Chicago, 1984).
- [60] E. Poisson, *A Relativist 's Toolkit: The Mathematics of Black-Hole Mechanics*, (Cambridge University Press, Cambridge, 2004).
- [61] J. M. Bardeen, W. H. Press, and S. A. Teukolsky, “Rotating black holes: Locally nonrotating frames, energy extraction, and scalar synchrotron radiation,” *Astrophys. J.* **178**, 347 (1972).
- [62] R. M. Wald, “Energy Limits on the Penrose Process,” *Astrophys. J.* **191**, 231 (1974).
- [63] G. Darrois, *Les équations de la gravitation Einsteinienne*, vol. XXV of *Mémorial des sciences mathématiques* (Gauthier-Villars, Paris, 1927).
- [64] W. Israel, “Singular hypersurfaces and thin shells in general relativity,” *Nuovo Cim. B* **44**, 1 (1966), Erratum: [*Nuovo Cim. B* **48**, 463 (1967)].
- [65] K. i. Nakao, H. Okawa, and K. i. Maeda, “Non-linear collisional Penrose process: How much energy can a black hole release?,” *PETP* **2018**, 013E01 (2018).